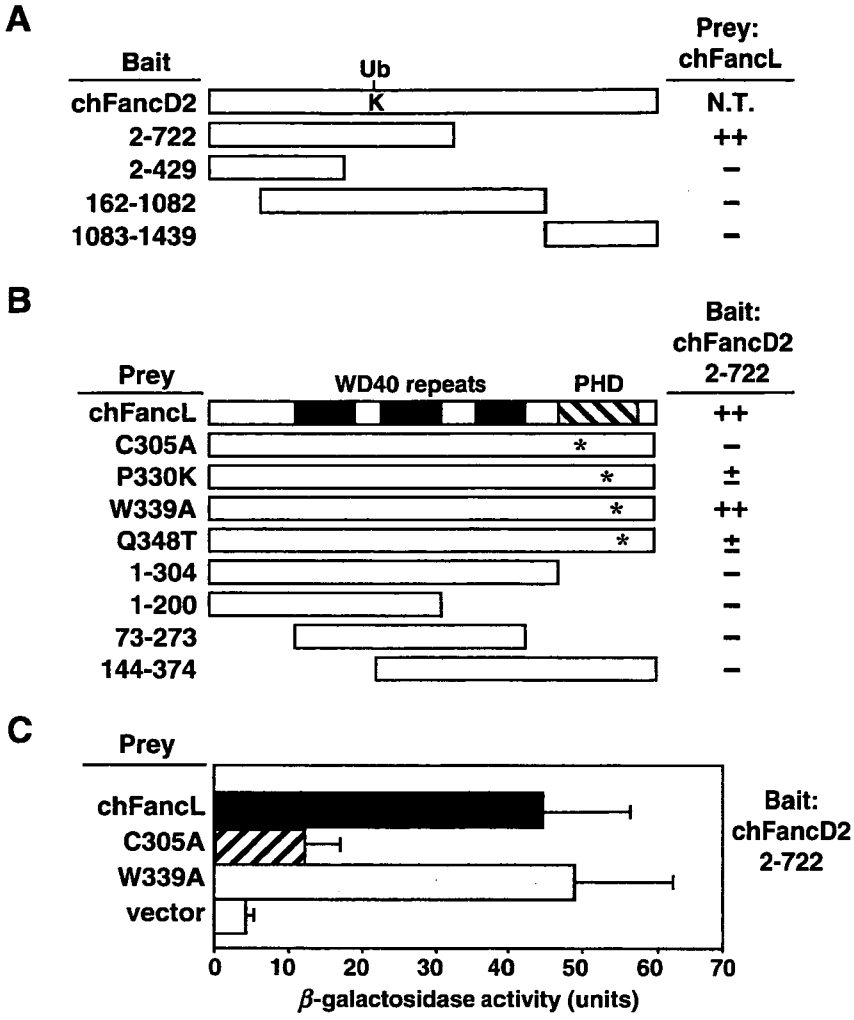

Figure 2 Interaction between chFancD2 and chFancL by Y2H analysis. Yeast cells were co-transformed with the bait plasmid containing a chFancD2 fragment and the prey plasmid containing a chFancL fragment. Activation of *LEU2* and *lacZ* reporter genes is shown in a semiquantitative way: ++, strong growth and blue colonies; ±, very weak growth and pale blue colonies; −, no growth and white colonies; N.T., not testable because of the autoactivation of reporters. (A) chFancD2 fragments used as a bait plasmid for assay with full-length chFancL prey plasmid as indicated. (B) chFancL fragments used as prey plasmid for assay with the chFancD2 2-722 bait plasmid. (C) β-galactosidase activity was determined using a liquid assay and calculated in Miller units. Yeast with the chFancD2 2-722 bait plasmid and the prey containing chFancL or its mutant (C305A or W339A) were used. Empty prey plasmid was included as a control. The data shown are means ± standard deviation (SD) of three independent transfectants.

line DT40. Based on the cDNA sequence, we PCR-amplified genomic DNA fragments of *chFANCL* and designed the targeting construct (Fig. 3A). The gene targeting was achieved by serial transfections with the construct, and gene disruption was verified by Southern (Fig. 3B) and Northern blot analyzes (Fig. 3C).

We first looked at the monoubiquitination of FancD2 in *fancl* cells. As shown in Fig. 3D, monoubiquitinated FancD2 (L-form) was markedly increased in intensity in response to MMC treatment in wild-type cells. In contrast, the L-form was not detected in *fancl* cells even after MMC treatment (Fig. 3D). This defect was restored by the expression of GFP-chFancL (Fig. 3D). Consistently, MMC-induced FancD2 focus formation was markedly decreased by *FANCL* disruption (see Fig. 5A, middle panel).

The DNA repair capacity of *fancl* cells was assessed using colony survival assays following exposure to DNA damaging agents. *fancl* cells were only slightly more sensitive to X-ray than were the wild-type controls (Fig. 3E), but were extremely sensitive to the DNA cross-linkers, cisplatin (as previously reported in Matsushita *et al.* 2005) and MMC (Fig. 3F). Again, the defects were complemented by the expression of GFP-chFancL in *fancl* cells (Fig. 3E,F, and Supplement Fig. S4C in Matsushita *et al.* 2005).

To test whether *fancl* cells have HR defects, we examined the frequencies of gene targeting events that occur at two independent genomic loci. Wild-type and *fancl* cells were transfected with gene targeting vectors in parallel, and targeting events were examined by Southern blot analysis. *FANCL*-deficient cells had a drastically reduced gene targeting efficiency compared to wild-type cells, and this defect was partially complemented by expression of GFP-chFancL (Table 2). These results indicate that *fancl* cells display phenotypes that are observed in other DT40 FA mutants, and that the severity of the defects is very similar to that seen in *fancd2-null* mutant cells (Yamamoto *et al.* 2005).

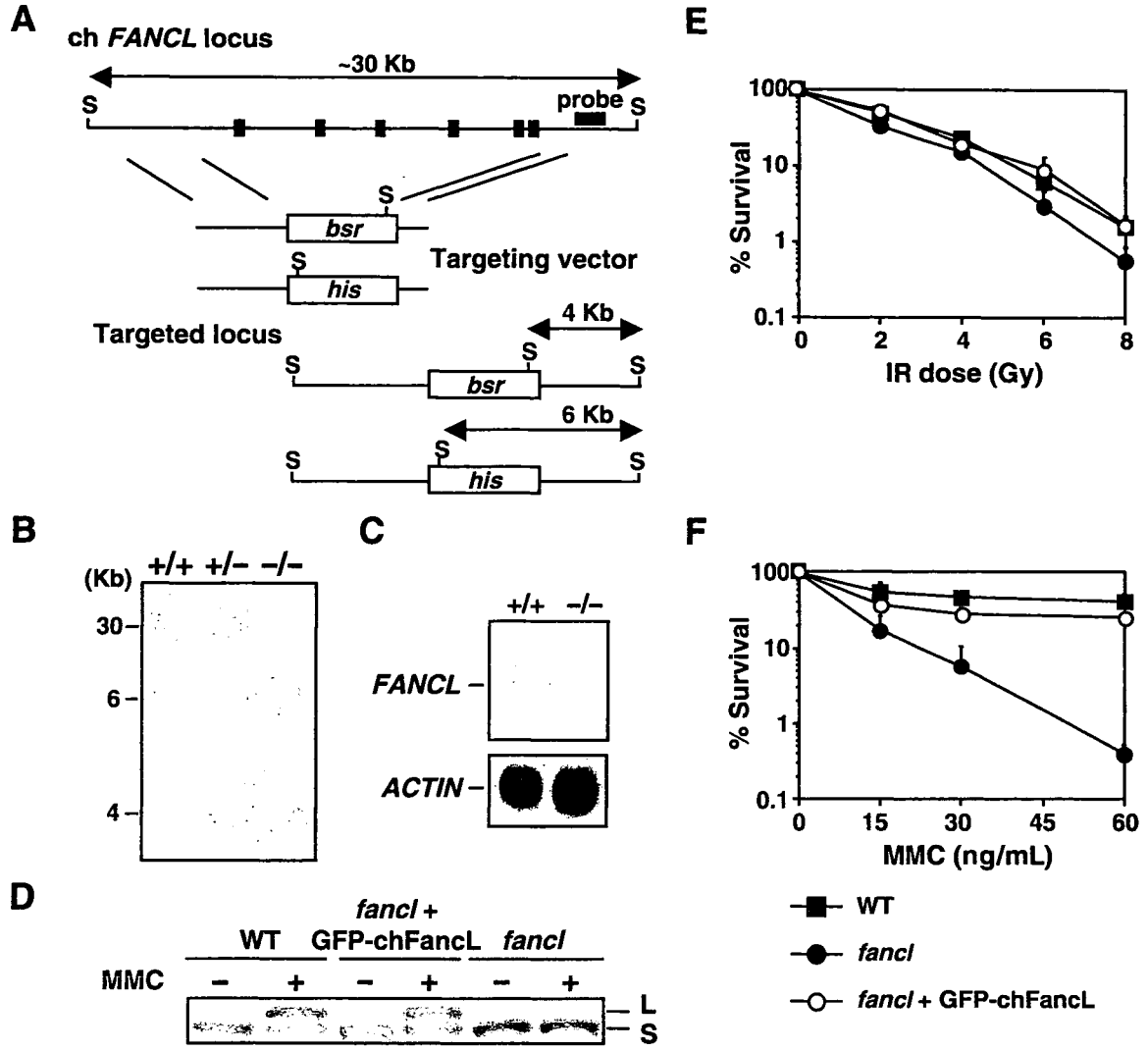

Figure 3 Targeted disruption of *chFANCL* loci in DT40 cells. (A) Schematic representation of partial *chFANCL* locus, the gene targeting constructs and the configuration of targeted alleles. The black box indicates the positions of exons that were disrupted. S, *Sac*I site. (B) Southern blot analysis of *Sac*I-digested genomic DNA from cells with indicated genotypes by using flanking probes as shown in panel A. (C) Northern blot analysis of total RNA from wild-type and *fancl* cells with a chFancL cDNA probe. (D) Western blot analysis of whole cell lysate prepared from wild-type, *fancl* and complemented *fancl* cells with GFP-chFancL expression vector using anti-chFancD2 sera. Cells were treated with MMC (500 ng/mL) for 6 h. L or S denotes the FancD2-L and FancD2-S forms, respectively. (E and F) Sensitivities of wild-type and *fancl* DT40 cells to DNA-damaging agents. The fraction of the surviving colonies following treatments with X-ray (E) or MMC (F) is shown. The data shown are means ± SD of at least three separate experiments.

Generation of FancD2 monoubiquitination site (K563R) mutant cells

In DT40 cells, it is quite straightforward to introduce a specific mutation into an endogenous locus by "knock-in" gene targeting. To examine the physiological significance of monoubiquitination of FancD2, we generated a *FANCD2* mutation in which the critical Lys residue was changed to Arg (*fancd2-K563R*). As summarized in (Fig. 4A,B), we first deleted three exons containing the monoubiquitination site in one allele by the *FANCD2-bsr* vector. Then the other allele was "knocked-in" with K563R mutation using *D2-K563R-his* vector. Finally, the *bsr* and *his* resistance gene cassettes were excised by GFP-Cre expression as described in Experimental procedures. Genotypes generated in each step in these procedures were verified by Southern blotting (Fig. 4C), and the mutation in *fancd2-K563R* cells was confirmed by DNA

Table 2 Targeted integration efficiencies in *fancl* cells

Genotype	Targeting vector	
	Ovalbumin-puro	*Xrcc2-puro*
wild-type	24/52 (46.2%)	7/22 (31.8%)
fancl	5/78 (6.4%)	1/65 (1.5%)
fancl + *GFP-chFANCL*	4/26 (15.4%)	2/20 (10.0%)

Shown are numbers of targeted colonies per total number of colonies analyzed by Southern blotting. The percentage of targeted integration events is given in parentheses.

sequencing of both PCR-amplified genomic DNA and transcripts (data not shown). Indeed, Western blotting showed that FancD2 L-form was not detected in *fancd2-K563R* cells before or after MMC treatment (Fig. 4D).

Direct comparison of *fancl*, *fancd2-null* and *fancd2-K563R* cells

We compared the phenotypes of *fancl*, *fancd2-null* and *fancd2-K563R* cells. First, we examined focus formation and chromatin targeting of FancD2 in *fancl* and *fancd2-K563R* cells. While wild-type cells displayed robust formation of FancD2 foci following MMC treatment, similarly treated *fancl* and *fancd2-K563R* cells could not form any significant levels of FancD2 foci (Fig. 5A). In wild-type cells, the FancD2 L-form was found to be targeted to chromatin after MMC treatment; however, both S- and L-forms in *fancl* and *fancd2-K563R* cells were not significantly localized in chromatin fraction (Fig. 5B). These results were consistent with the notion that chFancD2 was monoubiquitinated at K563 site, which was most likely catalyzed by chFancL. We next carried out cell growth analysis in parallel, and found that *fancl*, *fancd2-null* and *fancd2-K563R* cells displayed a similarly reduced growth rate compared to wild-type cells (Fig. 6A). We also found that the plating efficiency of these mutants was comparable (~30%), but was reduced relative to that of wild-type cells (nearly 100%).

It is known that FA mutant cells have defects in HR-mediated repair of DSBs (Yamamoto *et al.* 2003, 2005; Nakanishi *et al.* 2005). To directly test whether *fancl*, *fancd2-null* and *fancd2-K563R* mutant cells displayed differences in HR repair capacity, we carried out an assay for HR-mediated repair of an I-*Sce*I-induced DSB. Wild-type, *fancl*, *fancd2-null* and *fancd2-K563R* mutant cells that have the artificial recombination substrate SCneo integrated at the *OVALBUMIN* locus were used for this assay. A chromosomal DSB was introduced in one of the two tandem non-functional *neo* genes by transient introduction of an I-*Sce*I-encoding plasmid. A functional *neo* gene can be reconstituted if the DSB is repaired by HR using another partial *neo* gene as a template. Thus, HR-directed DSB repair capacity could be measured by counting the number of G418-resistant colonies (Yamamoto *et al.* 2003). The reduction in HR efficiency was 26, 24 and 30-fold in *fancd2-null*, *fancd2 K563* and *fancl* mutants, respectively, compared to the wild-type control (Fig. 6B). There were no statistically significant differences amongst the mutant cells. These results suggest that FancD2 monoubiquitination is essential for the activity of FancD2 in HR-mediated repair, and that the FancD2 K563R mutant protein has essentially no residual activity for the repair of chromosomal DSBs by HR.

Next, we examined the cross-linking sensitivity of these mutant cells using a colony formation assay in the presence of cisplatin (Fig. 6C) or following brief exposure to MMC (Fig. 6D). *Fancd2-null* and *fancd2-K563R* mutants showed almost the same level of sensitivity to these cross-linking agents, indicating that the cross-link repair function of FancD2 depends on its monoubiquitination. In contrast, *fancl* cells were slightly, but significantly, more sensitive than either *fancd2-null* or *fancd2-K563R* cells.

Discussion

To date, only FancE has been reported to directly interact with FancD2 among the FA core complex components (Medhurst *et al.* 2001; Pace *et al.* 2002; Gordon & Buchwald 2003). In this study, we have identified chicken PHF9/FancL as a FancD2-interacting protein by Y2H screening, and confirmed that by co-immunoprecipitation between ectopically expressed proteins. We suggest that the interaction between endogenous proteins should be weak and transient, and thus could be undetectable, since purified FA core complex containing FancL does not have FancD2 protein as its stable component (Meetei *et al.* 2003b). Nonetheless, our observation reinforces the notion that FancL monoubiquitinates FancD2 in a direct manner, although this has not been clearly established by *in vitro* reconstitution experiments.

We also found that any partial deletion of FancL or some of the tested point mutations in the PHD domain abrogated the interaction (Fig. 2), indicating that at least the PHD domain and the N-terminal 1-143 region are required to interact with chFancD2. hFancL C307A mutation also disrupted interactions with hFancA and hFancF (Table 1). As we have previously described, the equivalent chicken C305A mutation abrogated the capacity of the GFP-chFancL protein to complement

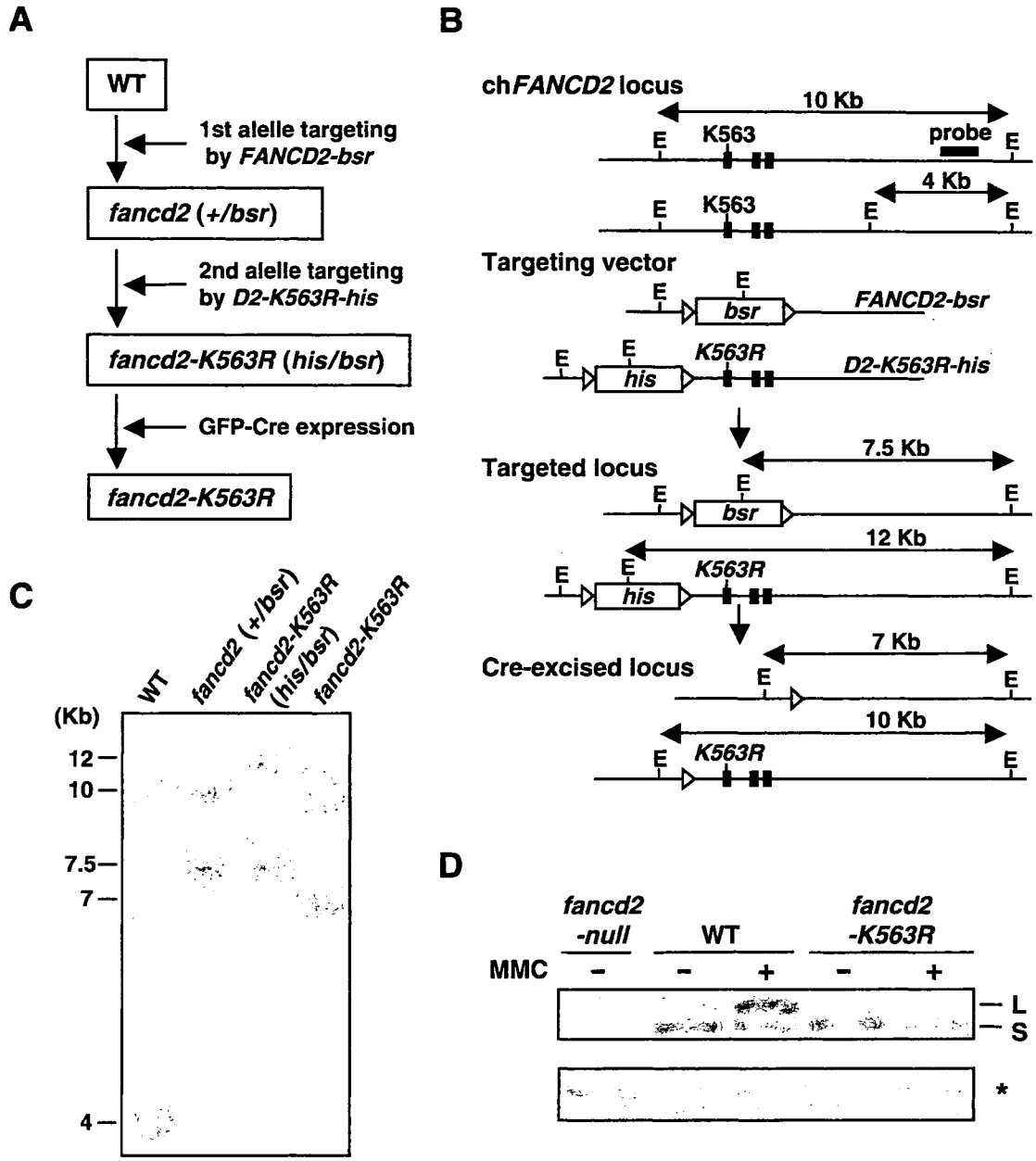

Figure 4 Generation of *fancd2-K563R* "knock-in" cells. (A) A strategy for making *fancd2-K563R* cells as described in Experimental procedures. The drug-resistant gene cassettes, which contain a loxP site at both ends, were removed by GFP-Cre expression and subsequent clone-sorting. (B) Schematic representation of partial chFancD2 locus, the gene targeting constructs and the configuration of targeted alleles. The black box indicates the positions of exons. The white arrowhead indicates the loxP site. E, *Eco*RI site. (C) Southern blot analysis of *Eco*RI-digested genomic DNA from cells with indicated genotypes by using flanking probes as shown in panel B. (D) Western blot analysis of whole cell lysate prepared from wild-type and *fancd2-K563R* cells with or without MMC treatment, as in Fig. 3D. Asterisk indicates nonspecific band as loading control of the samples.

cisplatin sensitivity as well as chromatin localization when expressed in *fancl* cells (Matsushita *et al.* 2005). Consistent with these results, a previous study reported that the human mutation (C307A) disrupted co-immunoprecipitation with hFancA, the ability to complement *fancl* patient's cells with FancD2 monoubiquitination and *in vitro* auto-ubiquitination activity (Meetei *et al.* 2003a). Thus this mutation likely disrupts multiple aspects of FancL function,

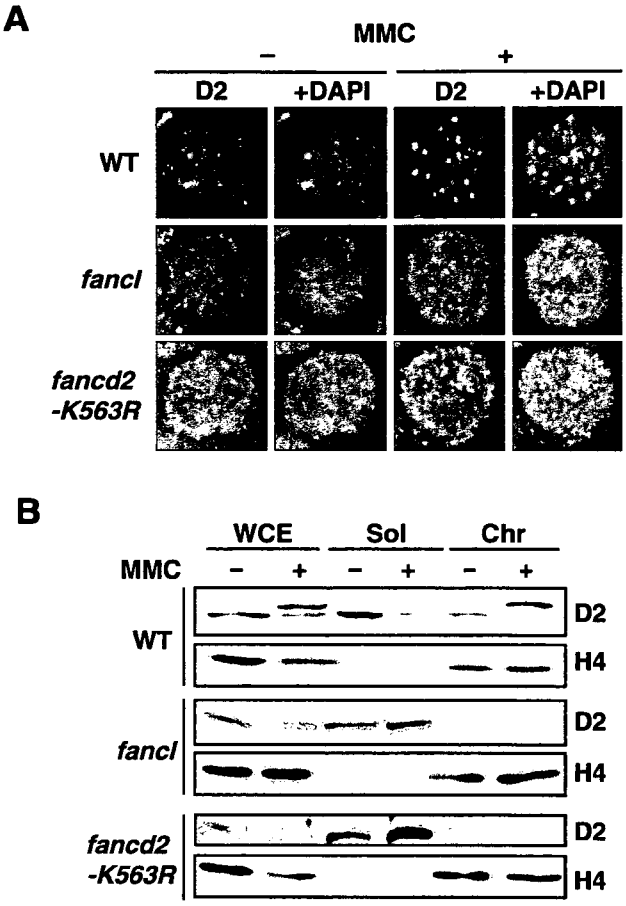

Figure 5 Characterization of *fancd2-K563R* cells. (A) FancD2 focus formation after MMC (500 ng/mL, 6 h) treatment. Cytospin slides were prepared, stained with anti-chFancD2 antibody followed by FITC-conjugated secondary antibody (Invitrogen) and DAPI, and observed under TCS-SP2 confocal laser-scanning microscope (Leica Microsystems, Wetzler, Germany). (B) Chromatin targeting of FancD2 protein. Cells were treated with MMC (500 ng/mL, 6 h) or left untreated, and then fractionated. Each fraction was separated by SDS-PAGE, and Western blotting was carried out using anti-chFancD2 or anti-Histone H4 (Upstate, Lake Placid, NY). WCE, whole cell extract; Sol, soluble fraction; Chr, chromatin fraction. Each lane of WCE, Sol, or Chr fractions contain proteins extracted from 100 thousand, one million, or two million cells, respectively.

including maintenance of the integrity of the core complex as well as ubiquitin E3 ligase activity. It would be interesting to test other mutations in a similar manner to dissect functions of FancL protein.

We have provided evidence of roles for FancL in ICL repair and HR. These functions were not unexpected, given the proposed role of FancL in the monoubiquitination and activation of FancD2. Several studies have implicated the monouibiquitination as a critical modification for activation of FancD2 for DNA repair. For example, mutant FancD2 protein lacking the monoubiquitination site abolished these functions when expressed in *FANCD2*-deficient PD20 cells (Garcia-Higuera *et al.* 2001; Taniguchi *et al.* 2002b). However, such ectopic expression does not necessarily provide definitive proof for a physiological role of the monoubiquitination, since this may lead to overproduction of FancD2. Furthermore, the endogenous *cis* element could be crucial for regulation of *FANCD2*, since defective immunoglobulin gene conversion in *fancd2* cells could not be complemented by CMV promoter-driven expression of FancD2 (Yamamoto *et al.* 2005). Similarly, the defects in targeted integration frequencies could not be fully complemented in both *fancd2* (Yamamoto *et al.* 2005) and *fancl* (this study) by expression of the corresponding expression vectors.

To more rigorously test the role of monoubiquitination (as well as FancL) for FancD2 activation, we generated *fancd2-K563R* cells and compared these cells with *fancd2-null* and *fancl* mutants. We found that *fancd2-K563R* and *fancd2-null* mutants displayed essentially the same degree of defects in cell growth, HR-mediated chromosomal DSB repair, and cisplatin and MMC sensitivity, indicating that absence of monoubiquitination functionally equates to absence of the protein. Thus, the monoubiquitination is critically important for FancD2 to function, at least in the assays analyzed here.

In cell growth and HR-directed DSB repair assays, the *fancl* and *fancd2* mutants showed a similar degree of impairment. In contrast, *fancl* cells showed consistently more severe cross-linking agent sensitivity compared to the other two *fancd2* mutants. Since two independently derived *fancl* clones (data not shown) were both more sensitive to cross-linkers than were the *fancd2* mutants, it seems unlikely that these results were due to simple clonal variation. This raises the following two possibilities. First, it is possible that FancL may ubiquitinate another substrate that modulates ICL repair, but not HR. Absence of FancL affects the function of this putative substrate as well as that of FancD2, and therefore the level of cisplatin sensitivity in *fancl* cells is the combined effects of the failure of two modifications. Alternatively, or additionally, *FANCL* mutation may disrupt the core complex, which will have the effect of disrupting the DNA repair activity mediated by the core complex. Based on our data using FancD2-fusion proteins, we have proposed that the core complex has its own role in DNA repair (Matsushita *et al.* 2005). FancM is an obvious candidate for an effector molecule of the core complex because of its potential DNA modifying activity. For example, *FANCL* mutation

Hsp90 regulates the Fanconi anemia DNA damage response pathway

Tsukasa Oda,[1] Toshiya Hayano,[2] Hidenobu Miyaso,[3] Nobuhiro Takahashi,[2] and Takayuki Yamashita[1]

[1]Laboratory of Molecular Genetics, Department of Molecular and Cellular Biology, Institute for Molecular and Cellular Regulation, Gunma University, Maebashi, Gunma, Japan; [2]Department of Applied Biological Science, Tokyo University of Agriculture and Technology, Fuchu, Tokyo, Japan; [3]Department of Bioenvironmental Medicine, Graduate School of Medicine, Chiba University, Chuo-ku, Chiba, Japan

Heat shock protein 90 (Hsp90) regulates diverse signaling pathways. Emerging evidence suggests that Hsp90 inhibitors, such as 17-allylamino-17-demethoxygeldanamycin (17-AAG), enhance DNA damage-induced cell death, suggesting that Hsp90 may regulate cellular responses to genotoxic stress. However, the underlying mechanisms are poorly understood. Here, we show that the Fanconi anemia (FA) pathway is involved in the Hsp90-mediated regulation of genotoxic stress response. In the FA pathway, assembly of 8 FA proteins including FANCA into a nuclear multiprotein complex, and the complex-dependent activation of FANCD2 are critical events for cellular tolerance against DNA cross-linkers. Hsp90 associates with FANCA, in vivo and in vitro, in a 17-AAG–sensitive manner. Disruption of the FANCA/Hsp90 association by cellular treatment with 17-AAG induces rapid proteasomal degradation and cytoplasmic relocalization of FANCA, leading to impaired activation of FANCD2. Furthermore, 17-AAG promotes DNA cross-linker–induced cytotoxicity, but this effect is much less pronounced in FA pathway-defective cells. Notably, 17-AAG enhances DNA cross-linker–induced chromosome aberrations. In conclusion, our results identify FANCA as a novel client of Hsp90, suggesting that Hsp90 promotes activation of the FA pathway through regulation of intracellular turnover and trafficking of FANCA, which is critical for cellular tolerance against genotoxic stress. (Blood. 2007;109: 5016-5026)

Introduction

Hsp90 is an abundant, evolutionarily conserved molecular chaperone whose function depends on its ability to bind and hydrolyze ATP. Through an ATPase cycle, Hsp90 facilitates proper folding of "client" proteins, thereby regulating their stability, protein interactions, intracellular trafficking, and functions.[1,2] To fulfill these functions, Hsp90 interacts with its cofactors and cochaperones including Hsp70, immunophilins, and p23, to form the Hsp90-based chaperone complex.[1,2] Natural compounds such as geldanamycin and radicicol bind the ATP-binding pocket of Hsp90 and disrupt its chaperone function.[3,4] Hsp90 is required for function and stability of diverse signal transduction proteins including oncogenic proteins such as ErbB2 and Raf-1.[2-7] Hence, the chaperone is an attractive target for cancer therapeutics. Indeed, Hsp90 inhibitors show antitumor activities in preclinical models, and geldanamycin analogues such as 17-allylamino-17-demethoxygeldanamycin (17-AAG) are currently undergoing clinical trials.[3,4] Importantly, Hsp90 inhibitors sensitize tumor cells to various genotoxic agents used for standard cancer therapeutics, including DNA cross-linkers,[8,9] ionizing radiation,[10] and replication inhibitors.[11,12] In line with these observations, it is suggested that Hsp90 regulates cell cycle checkpoints and DNA repair,[11-13] but the underlying mechanisms are poorly understood.

Fanconi anemia (FA) is a genetically heterogeneous inherited disorder characterized by progressive bone marrow failure, cancer susceptibility, and cellular hypersensitivity to DNA cross-linkers such as mitomycin C (MMC).[14-16] Multiple FA proteins cooperate in a common biochemical pathway, termed the FA pathway, which is involved in cellular response to DNA damage. At least 8 FA proteins, specifically, FANCA, FANCB, FANCC, FANCE, FANCF, FANCG, FANCL/PHF9, and FANCM, form a nuclear multiprotein complex (FA core complex), which is required for FANCD2 monoubiquitination in response to DNA damage.[17-32] DNA cross-linkers and replication inhibitors such as hydroxyurea (HU) are potent inducers of FANCD2 monoubiquitination.[14-16] The monoubiquitinated form of FANCD2 is targeted to the chromatin and participates in maintenance of genomic stability interacting with BRCA1 and BRCA2/FANCD1, at least in part, through homology-directed repair.[25,33-35] FANCJ/BRIP1, previously identified as a BRCA1-interacting helicase, may function downstream of FANCD2 activation or independently of the FA pathway.[36-38] Previous studies suggested that nuclear levels of FANCA have profound effects on FA core complex formation.[17-20,24,25,27] Nuclear levels of FANCA are determined by protein synthesis, degradation, and nucleocytoplasmic shuttling mediated by a bipartite nuclear localization signal (NLS) and 3 leucine-rich nuclear export signals.[18,39,40] However, little is known about the regulatory mechanisms for intracellular turnover and trafficking of FANCA.

In an attempt to elucidate the molecular mechanisms of the FA pathway, we found that Hsp90 was included in the FANCA-containing protein complex. The goal of the present study was to elucidate the molecular basis and functional significance of this interaction. We here provide evidence indicating that Hsp90 functions as a chaperone of FANCA and that Hsp90 promotes activation of the FA pathway through regulation of FANCA, which is critical for cellular tolerance to DNA cross-linkers. These

Submitted August 1, 2006; accepted November 2, 2006. Prepublished online as *Blood* First Edition Paper, February 27, 2007; DOI 10.1182/blood-2006-08-038638.

The publication costs of this article were defrayed in part by page charge payment. Therefore, and solely to indicate this fact, this article is hereby marked "advertisement" in accordance with 18 USC section 1734.

findings reveal that the FA pathway is involved in the Hsp90-mediated regulation of DNA damage response.

Materials and methods

Plasmids

Human FANCA cDNA with a FLAG-HA tandem-tag at the N-terminus (FH-FANCA) was inserted into a retroviral expression vector pLPCX (Clontech, Palo Alto, CA). An expression vector for HA-tagged ubiquitin was previously described.[25] Human FANCA cDNA and FANCG cDNA were cloned into pcDNA3 Myc vector[41] or pcDNA3 (Invitrogen, Carlsbad, CA).

Cell culture and transfections

FANCA-null SV40-immortalized fibroblasts GM6914, MCF7, 293T, NIH3T3, and HeLa cells were maintained in Dulbecco modified Eagle medium (DMEM) containing 10% fetal bovine serum. K562, Jurkat, and RPMI8226 cells were cultured in RPMI1640 medium supplemented with 10% fetal bovine serum. HeLa cells stably expressing FH-FANCA (HeLa/FH-FANCA cells) were obtained using a recombinant retrovirus as described previously.[27] A clone with appropriate expression of FH-FANCA (~5-fold of endogenous FANCA) was used for the present study. GM6914 cells stably expressing FANCA proteins were generated as described previously.[20,27] For transient expression, subconfluent HeLa cells were transfected with FuGENE 6 (Roche Diagnostics, Pleasanton, CA) according to the manufacturer's protocol. Hsp90 small interfering RNA (siRNA) was designed and transfected into HeLa cells using Lipofectamine 2000 (Invitrogen), as described.[42]

Antibodies

The antibodies used in this study were as follows: mouse monoclonal anti-Hsp90, which recognizes both Hsp90 α and Hsp90 β (F-8, Santa Cruz Biotechnology, Santa Cruz, CA); mouse monoclonal anti-Hsp90 β (SPA-843, StressGen, Victoria, BC, Canada); rabbit polyclonal anti-Hsp90 α (SPS-771, StressGen); mouse monoclonal anti-Hsp70 (SPA-810, StressGen); rabbit polyclonal anti-FANCD2 (Novus Biologicals, Littleton, CO); rabbit polyclonal antiubiquitin (SPA-200, StressGen); mouse monoclonal anti-HA (6E2, Cell Signaling Technology, Beverly, MA); mouse monoclonal anti-FLAG (M2, Sigma, St Louis, MO); mouse monoclonal anti-p23 (JJ3, Affinity Bioreagents, Golden, CO); mouse monoclonal anti–tubulin-β (TBN06, NeoMarkers, Fremont, CA); mouse monoclonal anti–γ-H2AX (JBW301, Upstate Cell Signaling Solutions, Charlottesville, VA); rabbit polyclonal anti-H2AX (Upstate Cell Signaling Solutions); mouse monoclonal anti-Myc (9E10, Santa Cruz Biotechnology); rabbit polyclonal anti-CHIP (Calbiochem, San Diego, CA); and mouse monoclonal anti–topoisomerase II (Transduction Laboratories, Lexington, KY). Rabbit polyclonal anti-FANCG (a gift from Dr J. P. de Winter, VU Medical Center, Amsterdam, The Netherlands),[22] rabbit polyclonal anti-FANCF (a gift from Dr M. E. Hoatlin, Oregon Health and Science University, Portland, OR),[43] rabbit polyclonal anti-FANCL and rabbit polyclonal anti-FANCM (gifts from Dr W. Wang, National Institutes of Health, Bethesda, MD),[29,31] rabbit polyclonal anti-FANCC,[19] and rabbit polyclonal anti-FANCA[19] antibodies were previously described.

Protein identification by liquid chromatography-tandem mass spectrometry analysis

HeLa/FH-FANCA cells were washed with ice-cold phosphate-buffered saline (PBS) and lysed in lysis buffer (50 mM Tris-HCl, pH 7.5, 150 mM NaCl, 0.5% NP-40, 5 mM Na_3VO_4, 5 mM NaF) containing a protease inhibitor cocktail (Roche Diagnostics) for 1 hour. After centrifugation at 16 000*g* for 30 minutes at 4°C, the supernatants were incubated with anti-FLAG M2-agarose at 4°C for 6 hours. After extensive washing, the bound complexes were eluted with Tris-buffered saline containing 0.1 mg/mL of the FLAG peptide (Sigma) and digested with endoproteinase Lys-C. The resulting peptides were analyzed by a liquid chromatography-tandem mass spectrometry (LC-MS/MS) system at the femtomole level as described.[44,45]

Immunoprecipitation and immunoblot analysis

Immunoprecipitation and immunoblotting were performed as described previously.[27] For detection of polyubiquitinated FANCA, cells were lysed in ubiquitin lysis buffer (50 mM Tris-HCl, pH 8.0, 150 mM NaCl, 1% Triton X-100, 0.2% Sarkosyl) supplemented with 5 mM *N*-ethylmaleimide, 1 mM dithiothreitol, 2 mM Na_3VO_4, 5 mM NaF, and a protease inhibitor cocktail. Immunoprecipitated proteins and cell lysates were subjected to sodium dodecyl sulfate-polyacrylamide gel electrophoresis (SDS-PAGE). Quantification of protein signals was performed by densitometry using National Institutes of Health Image software.

Immunofluorescence microscopy

Cells were immunostained as described previously.[27] Cell nuclei were stained with a mounting medium containing 4′, 6-diamidino-2-phenylindole (DAPI; Vector Laboratories, Burlingame, CA). Fluorescence microscopy was performed as described previously.[27]

Subcellular fractionation

Cytoplasmic and nuclear fractions were prepared from HeLa cells using CelLytic NuCLEAR extraction kit (Sigma) according to the manufacturer's protocol. Cytoplasmic and nuclear extracts were prepared as described.[27]

In vitro binding assay

Myc-FANCA, Myc-FANCG, and FANCA proteins were expressed in rabbit reticulocyte lysates (RRLs) using the TNT T7 Quick Coupled Transcription/Translation System (Promega, Madison, WI) according to the supplier's instructions. In vitro transcription/translation reactions were performed in a total volume of 50 μL for 90 minutes at 30°C, using pcDNA3 plasmids encoding the proteins. Reaction mixture was diluted with 500 μL HEPES buffer (10 mM HEPES, pH 7.6, 150 mM KCl, 10 mM $MgCl_2$, 5 mM NaF, 20 mM Na_2MoO_4, 0.1% NP40) and the synthesized Myc-FANCA and Myc-FANCG were immunoprecipitated with an anti-Myc antibody, followed by immunoblot analyses. FLAG-tagged wild-type and truncated polypeptides of FANCA were synthesized in vitro, using DNA templates containing the T7 promoter and corresponding nucleotide sequences, and immunoprecipitated from the reaction using anti-FLAG antibody, followed by immunoblot analyses.

Cell survival assay

Cells were seeded in 6-well tissue culture plates at a density of 2×10^5 cells/well and allowed to grow overnight, and then treated with drugs, as indicated. Cells were replated in 96-well tissue culture plates at a density of 5×10^3 cells/well, and then incubated with drug-free culture medium to complete a total 72 hours from the time of initial drug application. Cell survival was colorimetrically measured using 4-[3-(4-iodophenyl)-2-(4-nitrophenyl)-2*H*-5-tetrazolio]-1,3-benzene disulfonate assay kit (Dojindo Molecular Technologies, Gaithersburg, MD) as described.[27]

TUNEL staining

Drug-treated cells were replated into 8-well chamber slides (Electron Microscopy Science, Fort Washington, PA) at a density of 2×10^4 cells/well and incubated in drug-free culture medium, as indicated. Cells were fixed in fresh 4% paraformaldehyde for 25 minutes followed by permeabilization with 0.3% Triton X-100 in PBS for 5 minutes. TdT-mediated dUTP nick-end labeling (TUNEL) staining was performed with a detection kit (Roche Diagnostics).

Chromosome breakage analysis

HeLa cells were treated with drugs for 24 hours and Colcemid (Gibco BRL, Carlsbad, CA) for the last 3 hours. Cells were swollen using 0.075 M KCl

and fixed with methanol-acetic acid (3:1). Slides were stained with Giemsa and 50 to 100 metaphases were examined.

Results

Hsp90 associates with FANCA in vivo

To elucidate regulatory mechanisms of the FA core complex, we conducted LC-MS/MS analysis of FANCA-containing protein complexes immunopurified from HeLa/FH-FANCA cells. We identified 96 potential FANCA-associated proteins after subtracting proteins in the immunoprecipitated fraction from mock-transfected cells. This experiment was validated by detection of known FANCA-associated proteins—that is, FANCG,[20,22] FANCB,[30] FANCL,[29] and BLM.[46] Among the potential FANCA-associated proteins, Hsp90 α and Hsp90 β were the major components. The association of Hsp90 with FANCA was confirmed by immunoblotting analysis and reciprocal immunoprecipitation followed by immunoblotting (Figure 1A, lanes 1-4). In similar studies, the association of FANCA with both isoforms of Hsp90 was confirmed (data not shown). Moreover, in parental HeLa cells (Figure 1A, lanes 5-8) and K562 human myeloid leukemic cells (data not shown), endogenous FANCA associated with Hsp90 and its cochaperone p23, which preferentially binds to an ATP-bound form of Hsp90, stabilizing the interaction between Hsp90 and its client proteins.[2] In addition, Hsp70 coimmunoprecipitated with endogenous FANCA in these cells (data not shown). These data suggest that the Hsp90-based chaperone complex[1,2] associates with FANCA.

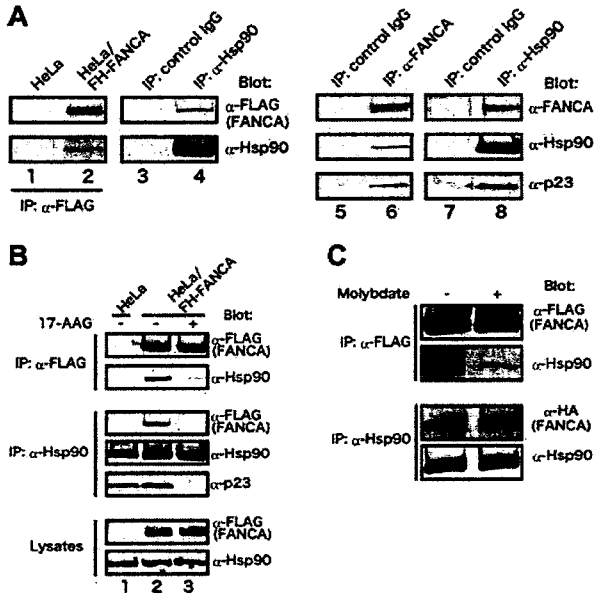

Figure 1. Hsp90 specifically associates with FANCA in vivo. (A) Coimmunoprecipitation of Hsp90 with FANCA. Lysates from control HeLa cells and HeLa/FH-FANCA cells were immunoprecipitated (IP) with anti-FLAG antibody and immunoblotted with anti-FLAG and anti-Hsp90 antibodies (lanes 1 and 2). Reciprocally, lysates from HeLa/FH-FANCA cells were immunoprecipitated with either control mouse IgG or mouse anti-Hsp90 monoclonal antibody and immunoblotted with anti-FLAG and anti-Hsp90 antibodies (lanes 3 and 4). Lysates from HeLa cells were immunoprecipitated with either control rabbit IgG or anti-FANCA and immunoblotted with the indicated antibodies (lanes 5 and 6), or immunoprecipitated with either control mouse IgG or anti-Hsp90 antibody and immunoblotted with the indicated antibodies (lanes 7 and 8). (B) Inhibition of the interaction between FANCA and Hsp90 by 17-AAG. HeLa/FH-FANCA cells were treated with vehicle (−) or 250 nM 17-AAG (+) for 15 minutes (lanes 2 and 3). Vehicle-treated parental HeLa cells were used as control (lane 1). Lysates from these cells were immunoprecipitated with anti-FLAG antibody and immunoblotted with the indicated antibodies (upper panels), or were immunoprecipitated with anti-Hsp90 antibody and immunoblotted with the indicated antibodies (middle panels). Lysates were directly immunoblotted with the indicated antibodies to confirm that FH-FANCA and Hsp90 protein levels were constant after 17-AAG treatment (lower panels). (C) Stabilization of the interaction between FANCA and Hsp90 by molybdate. HeLa/FH-FANCA cells were lysed in a buffer (10 mM HEPES, pH 7.5, 10 mM $MgCl_2$, 150 mM KCl, 0.2% Tween 20) in the presence (+) or absence (−) of 20 mM molybdate. Lysates were immunoprecipitated with anti-FLAG antibody and immunoblotted with the indicated antibodies (upper panels), or immunoprecipitated with anti-Hsp90 antibody and immunoblotted with the indicated antibodies (lower panels).

To test whether the FANCA/Hsp90 interaction was specific, we examined effects of 17-AAG and molybdate. 17-AAG disrupts the interaction between Hsp90 and its clients,[2-4] whereas molybdate stabilizes the interaction.[47,48] Our results showed that cellular treatment with 17-AAG induced a rapid dissociation between Hsp90 and FANCA (Figure 1B). As previously described,[49] 17-AAG disrupted the interaction between Hsp90 and p23 under the same conditions. Figure 1C shows that the FANCA/Hsp90 interaction was labile in a buffer without molybdate, whereas the interaction was prominently stabilized in the presence of molybdate (Figure 1C). Since vanadate has similar function,[48] our standard lysis buffer containing vanadate presumably made it easier to detect the Hsp90/FANCA complex. Collectively these results strongly suggest that the FANCA/Hsp90 interaction is associated with the chaperone activity of Hsp90.

Hsp90 inhibition induces proteasomal degradation and cytoplasmic redistribution of FANCA

To understand the functional significance of the association of Hsp90 with FANCA, we examined effects of 17-AAG on FANCA and other FA proteins included in the FA core complex in HeLa/FH-FANCA (Figure 2A) and parental HeLa (Figure 2B) cells. In both cells, FANCA was markedly down-regulated within 1 to 2 hours after cellular treatment with 17-AAG, whereas other FA proteins decreased gradually following rapid reduction in FANCA levels. The different kinetics of FANCA and FANCG decreases seemed to conflict with previous observations that the 2 proteins bind and stabilize each other, and that deficiency of either causes accelerated degradation of the other.[24] However, it should be noted that our experimental conditions were different from previous studies.[24] Most importantly, FANCA- and FANCG-deficient cells were used in the previous studies,[24] whereas effects of the drug-induced acute depletions of FANCA and FANCG were analyzed in the present study. Figure 2C shows that 17-AAG induced decreases of FANCA protein levels in HeLa cells and MCF7 human breast cancer cells, in a dose-dependent manner within the range of 50 to 500 nM, which was consistent with known effective doses of the drug.[50] The dramatic effect of 17-AAG on FANCA protein levels suggested that FANCA might be a client of Hsp90. To confirm that the effect of 17-AAG was not cell-type specific, we examined the effect of the drug in other cells. Following drug treatment, FANCA was markedly decreased in K562 cells, Jurkat human T-cell leukemia/lymphoma cells, RPMI8226 human myeloma cells, and NIH3T3 murine fibroblasts (Figure 2D, lanes 1-8). In addition, the structurally unrelated Hsp90 inhibitors radicicol and novobiocin,[4] showed similar effects on FANCA protein levels (Figure 2D, lanes 9-12), excluding nonspecific effects of 17-AAG. To confirm the effects of Hsp90 inhibitors, we tried to deplete Hsp90 by transient transfection of siRNA, but Hsp90 levels were only mildly reduced and FANCA protein levels were not affected (data not shown).

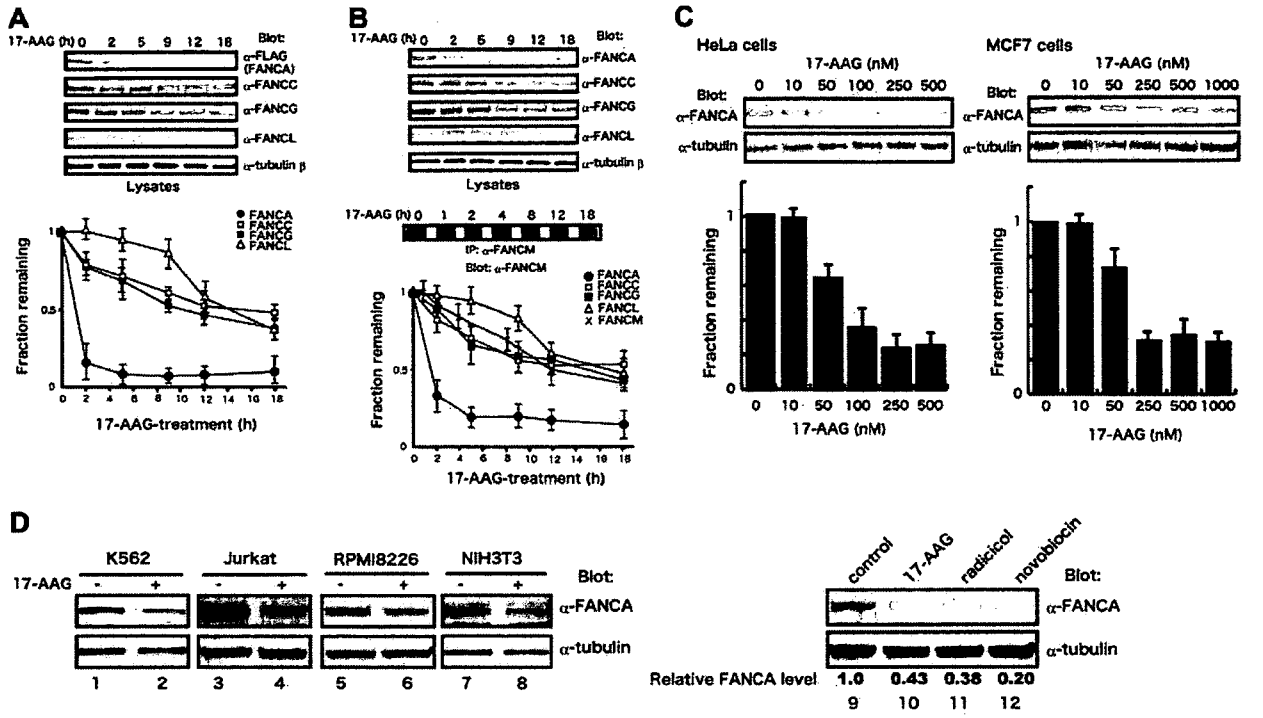

Figure 2. 17-AAG induces a rapid down-regulation of FANCA. HeLa/FH-FANCA (A) and parental HeLa (B) cells were treated with 250 nM 17-AAG for the indicated times. Lysates were immunoblotted with the indicated antibodies. To assess total cellular levels of FANCM, whole-cell lysates were immunoprecipitated (IP) and immunoblotted with anti-FANCM antibody. FA protein signals were quantified and normalized against tubulin-β signals. Data represent means ± SE from 3 independent experiments (bottom graphs). (C) Dose-dependent down-regulation of FANCA by 17-AAG. HeLa and MCF7 cells were treated with various concentrations of 17-AAG for 2 hours. Cell lysates were immunoblotted with the indicated antibodies (upper panels). FANCA signals were quantified and normalized against tubulin-β signals. Data represent means ± SD from 3 independent experiments (bottom graphs). (D) After treatment with vehicle (−) or 17-AAG (+), lysates from K562 cells (500 nM, 4 hours), Jurkat cells (250 nM, 2 hours), RPMI8226 cells (1 μM, 2 hours), and NIH3T3 cells (1 μM, 4 hours) were immunoblotted with appropriate antibodies (lanes 1-8). HeLa cells were treated with 250 nM 17-AAG, 2 μM radicicol, or 2 mM novobiocin for 2 hours (lanes 9-12). Cell lysates were immunoblotted with anti-FANCA and anti–tubulin-β antibodies. Numbers at the bottom of sample lanes 9-12 represent relative FANCA protein levels normalized against control.

Because 17-AAG is known to accelerate degradation of Hsp90-interacting clients, we assessed the effect of 17-AAG on stability of FANCA by monitoring FANCA protein levels after blocking protein synthesis (Figure 3A-B). The half-life of FANCA was about 8 hours in HeLa/FH-FANCA cells, whereas it was reduced to about 1 hour in 17-AAG–treated cells, suggesting that the drug accelerated degradation of FANCA (Figure 3A). Similarly, the half-life of endogenous FANCA was markedly reduced from about 8 hours to about 2 hours after 17-AAG treatment of parental HeLa cells (Figure 3B). We next examined effects of proteasome inhibitors. As shown in Figure 3C, MG132 and lactacystin inhibited 17-AAG–induced reduction of FANCA. Polyubiquitination precedes proteasomal degradation of a wide variety of proteins. We therefore examined the effect of 17-AAG on ubiquitination of FANCA. For this purpose, cell lysates of HeLa/FH-FANCA were immunoprecipitated using an anti-FLAG antibody, and immunoblotted with an antiubiquitin antibody. Drug treatment increased polyubiquitinated forms of FANCA, detected as a smear with slower mobility, particularly in the presence of MG132 (Figure 3D left panels). The presence of ubiquitinated FANCA in cells treated with MG132 alone suggested that FH-FANCA was ubiquitinated at basal states. To study ubiquitination of endogenous FANCA, we transiently transfected HeLa cells with HA-ubiquitin and treated the cells with 17-AAG or MG132 or both. FANCA was immunoprecipitated and immunoblotted with an anti-HA antibody. Consistent with the results obtained in HeLa/FH-FANCA, treatment with 17-AAG with or without MG132 promoted polyubiquitination of FANCA (Figure 3D right panels). Taken together, these results suggest that Hsp90 inhibition induces FANCA degradation through the ubiquitin-proteasome pathway.

Because Hsp90 inhibition promotes Hsp70-mediated association of several clients with the chaperone-associated ubiquitin ligase CHIP leading to their proteasomal degradation,[6,7,51] we studied its interaction with FANCA. Our results showed that interactions of CHIP with FANCA and Hsp70 were markedly enhanced after 17-AAG treatment in HeLa/FH-FANCA cells (Figure 3E). The proteasome inhibitor MG132 stabilized the CHIP-Hsp70-FANCA complex, in the absence and presence of 17-AAG. These results suggest that CHIP may be involved in the 17-AAG-induced proteasomal degradation of FANCA.

Nuclear localization of FANCA is critical for its function and appears to be regulated by its tertiary conformation of the C-terminus[18,27,39]; in addition, Hsp90 regulates transmembrane trafficking of some client proteins.[2] We therefore studied the effect of 17-AAG on subcellular localization of FANCA. Anti-HA immunostaining of HeLa/FH-FANCA cells (Figure 4A-D) showed that although transduced FANCA was predominant in the nucleus at basal states, as previously described,[18,20,27,39] it relocalized to the cytoplasm, particularly to the perinuclear cytoplasm after cellular exposure to 17-AAG (Figure 4C-D). Because FH-FANCA was reduced during drug treatment, exposure time for image acquisition was adjusted for optimal visualization of each specimen. Few signals were observed in the nuclei and the cytoplasm of control HeLa cells (Figure 4E), supporting the specificity of fluorescence signals in this system. To further confirm these results, GM6914

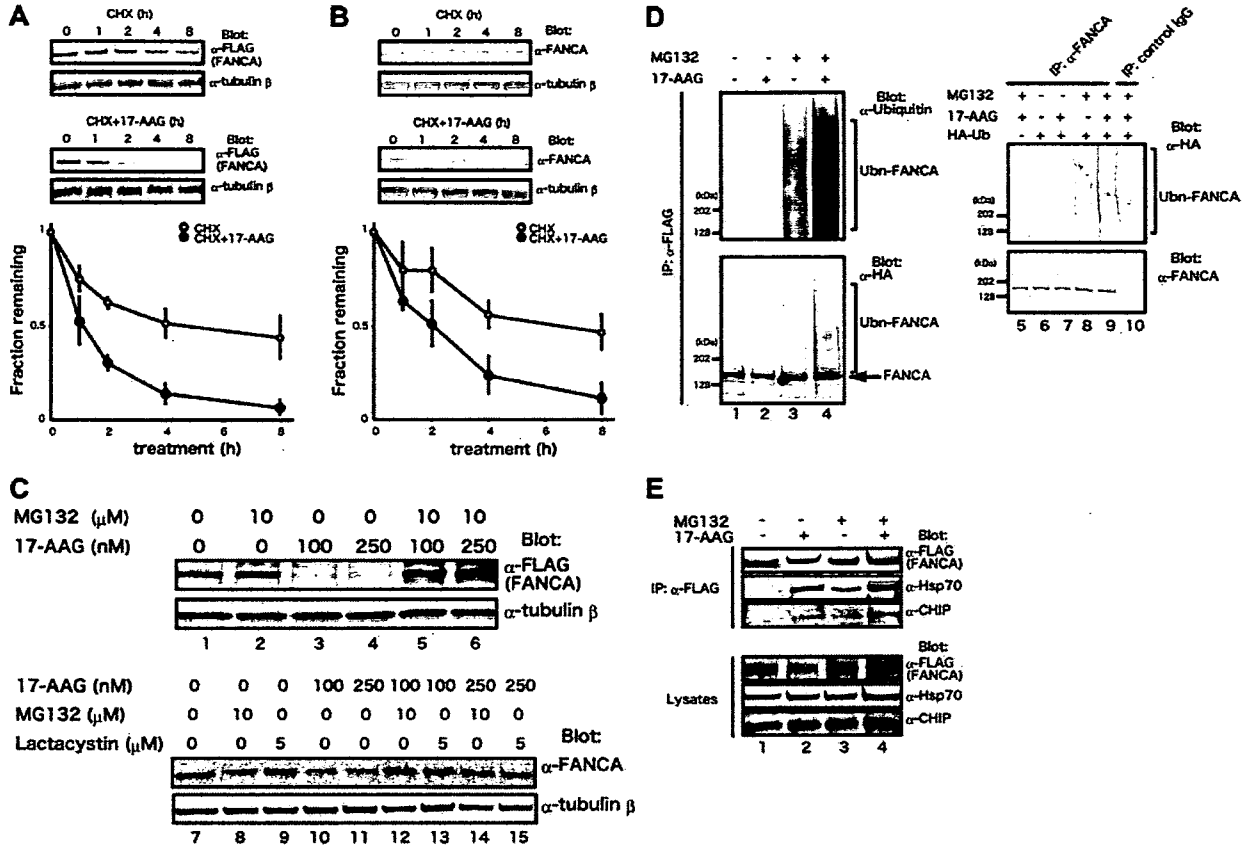

Figure 3. 17-AAG induces degradation of FANCA via the ubiquitin-proteasome pathway. (A-B) FANCA degradation induced by 17-AAG. HeLa/FH-FANCA (A) and parental HeLa (B) cells were treated with 100 μg/mL CHX alone (CHX) or with 250 nM 17-AAG (CHX + 17-AAG) for the indicated times. Cell lysates were immunoblotted with the indicated antibodies (upper blots). FANCA signals were quantified and normalized against tubulin-β signals. Data represent means ± SE from 3 independent experiments (bottom graphs). (C) Proteasome inhibitors block 17-AAG–induced FANCA down-regulation. HeLa/FH-FANCA cells were treated with 17-AAG or MG132, at appropriate concentrations for 4 hours (lanes 1-6). Cell lysates prepared using SDS-sample buffer were immunoblotted with anti-FLAG and anti–tubulin-β antibodies. HeLa cells were treated with 17-AAG and proteasome inhibitors, MG132 or lactacystin, at appropriate concentrations for 4 hours (lanes 7-15). Cell lysates prepared using SDS-sample buffer were immunoblotted with anti-FANCA and anti–tubulin-β antibodies. (D) Enhancement of polyubiquitination of FANCA by 17-AAG. HeLa/FH-FANCA cells were treated with vehicle (−) or 250 nM 17-AAG (+), in the absence (−) or presence (+) of 10 μM MG132 for 1 hour (lanes 1-4). Cell lysates prepared using ubiquitin lysis buffer were immunoprecipitated with anti-FLAG antibody and immunoblotted with antiubiquitin and anti-HA antibodies to detect polyubiquitinated FANCA (Ubn-FANCA). The arrow indicates nonubiquitinated FANCA. HeLa cells were transfected with empty vector (−; lane 5) or a plasmid encoding HA-ubiquitin (HA-Ub; +; lanes 6-10). After 24 hours of transfection, cells were treated with 17-AAG and MG132, as described. Cell lysates were immunoprecipitated with either anti-FANCA antibody (lanes 5-9) or control rabbit IgG (lane 10) and immunoblotted with anti-HA and anti-FANCA antibodies. (E) Association of CHIP with FANCA. HeLa/FH-FANCA cells were treated with 17-AAG and MG132 alone or in combination (lanes 1-4), as described in Figure 3D. Cell lysates were immunoprecipitated using anti-FLAG M2 agarose and immunoblotted with the indicated antibodies (upper panels). The same lysates were immunoblotted with the indicated antibodies (lower panels).

fibroblasts stably transduced with wild-type FANCA were immunostained with an anti-FANCA antibody, and again the drug-induced cytoplasmic relocalization of FANCA was observed (Figure 4F-G). Most of control GM6914 cells gave only a few background signals (Figure 4H).

Hsp90 stabilizes cytoplasmic FANCA independently of FANCG

To further characterize the interaction between Hsp90 and FANCA, we determined the subcellular localization of the FANCA/Hsp90 complex. Cell fractionation studies using HeLa/FH-FANCA cells (Figure 5A) showed that the FANCA/Hsp90 complex was mainly detectable in the cytoplasm, whereas the FANCA/C/F complex was predominant in the nucleus, as previously described.[20,23] Consistently, the association between Hsp90 and endogenous FANCA was mostly attributed to the cytoplasmic Hsp90/FANCA complex in parental HeLa cells (Figure 5B). These results suggest that the major target of Hsp90 is a cytoplasmic fraction of FANCA.

The FANCA/G complex is detectable in the cytoplasm probably as an early intermediate subcomplex during assembly of the FA core complex.[20,22,27,32] In addition, FANCG has a tetratricopeptide repeat domain,[52] which serves as an Hsp90-interacting consensus motif in various cochaperones.[1] Thus, it is hypothesized that Hsp90 directly binds to FANCG and stabilizes FANCA through promoting the FANCA/G interaction. To address this question, we expressed FANCA or FANCG by in vitro translation in RRL. RRL is a rich source of Hsp90 and its cofactors such as Hsp70 and p23, which form the Hsp90-based multichaperone complex. In these reactions, FANCA associated with Hsp90 in a 17-AAG–sensitive manner, whereas FANCG did not (Figure 5C upper panels). When FANCA and FANCG were cotranslated in RRL, the 2 proteins formed a complex, which was not affected in the presence of 17-AAG (Figure 5C lower panels). Thus, contrary to this hypothesis, the Hsp90 chaperone complex directly bound FANCA but not FANCG in vitro and had little effect on the FANCA/G interaction.

To determine the region of FANCA that was responsible for the interaction with Hsp90, we expressed a series of FANCA deletion mutants and examined their interactions with Hsp90 in the same system. As shown in Figure 5D, Hsp90 could interact with

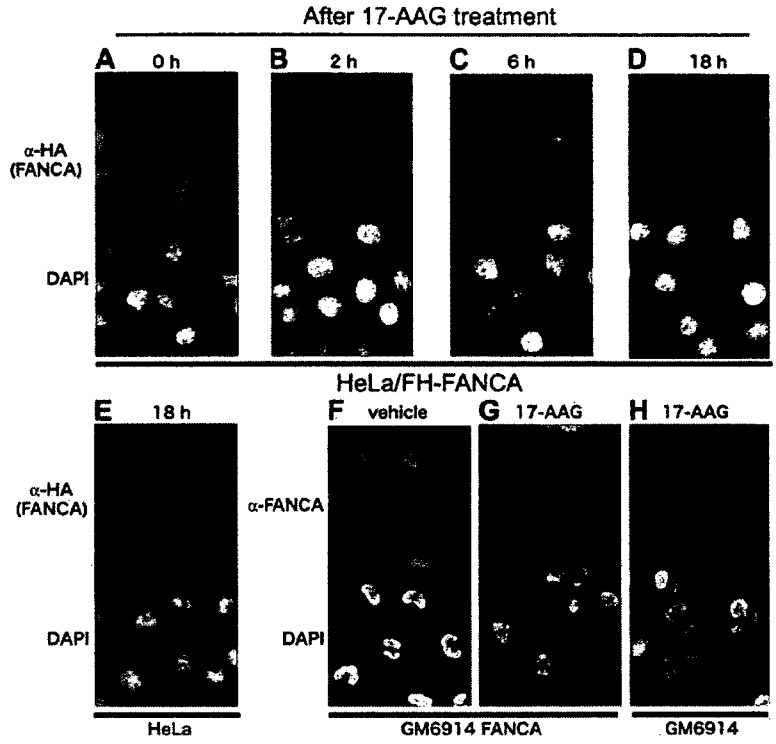

Figure 4. 17-AAG induces cytoplasmic relocalization of FANCA. HeLa/FH-FANCA cells (A-D) and control HeLa cells (E) were treated with 250 nM 17-AAG for the indicated times, and then stained with anti-HA antibody. GM6914 cells stably expressing wild-type FANCA (GM6914/FANCA) were cultured with vehicle (F) or 250 nM 17-AAG (G) for 18 hours, and then stained with anti-FANCA antibody. As a control, GM6914 cells treated with 250 nM 17-AAG for 18 hours were stained with anti-FANCA antibody (H). For optimal visualization of fluorescence signals, exposure time was adjusted. Cell nuclei were visualized with DAPI staining. Images were obtained on an Olympus AX70 microscope equipped with UPlan Apo 20×/0.70 NA and WH10×/22 lenses (Olympus, Tokyo, Japan) using a PXL charged-coupled device camera (model CH1; Photometrics, Osnabruck, Germany).

full-length, 1-1200, and 1-900 fragments of FANCA, whereas the binding of 1-600 FANCA to Hsp90 was drastically diminished, and no interaction was observed between 1-300 FANCA and Hsp90. The N-terminal deletion mutants 301-1455 and 601-1455 FANCA bound to Hsp90. The Hsp90-binding of 901-1455 and 1201-1455 FANCA was reduced and not observed, respectively. Further analysis showed that both of 601-900 and 901-1200 FANCA moderately bound to Hsp90, and 601-1200 FANCA intensely bound to Hsp90. Thus, both amino acid residues 601-900 and 901-1200 of FANCA are required for full binding to Hsp90. On the other hand, 1-300 of FANCA was responsible for binding to FANCG, consistent with previous reports.[20,21] These results suggest that Hsp90 and FANCG independently recognize different regions of FANCA.

In a further attempt to identify amino acid residues responsible for interaction with Hsp90, we examined association of Hsp90 with several patient-derived mutant proteins (H492R, H1110P, F1263del, and W1302R), in which mutations were located on and surrounding the Hsp90-binding fragments of FANCA. These mutants, expressed in GM6914 FANCA-null cells, fail to complement the cells and enter the nucleus. [27] However, these mutations markedly enhanced interaction between Hsp90 and FANCA (Figure 5E). Although these results may appear to be paradoxical to the notion that Hsp90 promotes FANCA, enhanced binding to client proteins with aberrant conformation is a physiologic behavior of the chaperone. Further work is required to elucidate the structural basis of the interaction between Hsp90 and FANCA. The previous observation that these mutant proteins interact with FANCG to a similar extent with the wild-type protein[27] further supports the notion that FANCG and Hsp90 independently interact with FANCA.

Taken together, these results suggest that Hsp90 stabilizes cytoplasmic FANCA in a FANCG-independent manner. To confirm this notion, we stably expressed ΔNLS FANCA mutant lacking an N-terminal region (amino acid residues 1-35) in GM6914 cells, and studied its turnover. The mutant protein fails to bind FANCG and fails to enter the nucleus.[18,20,39] The results showed that the ΔNLS mutant was degraded at a similar rate to wild-type FANCA (Figure 5E). Unexpectedly, the basal half-life of the ΔNLS mutant protein was also similar to the wild-type protein. One explanation is that FANCG-binding plays a minor role in the stability of the cytoplasmic pool, although it is required for maintaining total cellular levels of FANCA through stabilization of the FA core complex in the nucleus. Thus, Hsp90 and FANCG play distinct roles in cellular homeostasis of FANCA.

17-AAG suppresses activation of FANCD2

The 17-AAG–induced reduction and cytoplasmic relocalization of FANCA are expected to impair downstream activation of FANCD2 through depletion of the FA core complex in the nucleus. Therefore, we examined the effect of 17-AAG on FANCD2 monoubiquitination following cellular treatment with MMC. In HeLa cells, FANCD2 monoubiquitination began to increase 2 hours after MMC treatment, reaching a maximal plateau at 12 to 16 hours (Figure 6A). Addition of 17-AAG suppressed MMC-stimulated FANCD2 monoubiquitination, which was evident from 8 hours. It should be noted that 17-AAG treatment induced slow decrease in total FANCD2 levels, which may contribute to suppression of FANCD2 monoubiquitination in the late phase. A dose-response study showed that 17-AAG suppressed FANCD2 monoubiquitination at a similar range of concentrations (50-500 nM) to those where FANCA was down-regulated (data not shown). Moreover, the drug suppressed FANCD2 monoubiquitination in HU-treated cells (Figure 6C). FANCD2 monoubiquitination seems to be triggered by the formation of double-strand breaks (DSBs) during DNA replication after cellular exposure to DNA cross-linkers and replication inhibitors.[53] Thus, it could be possible that the 17-AAG–mediated suppression of FANCD2 activation was secondary to suppressed DSB formation due to the drug-induced growth arrest. To exclude this possibility, we examined the effect of 17-AAG on

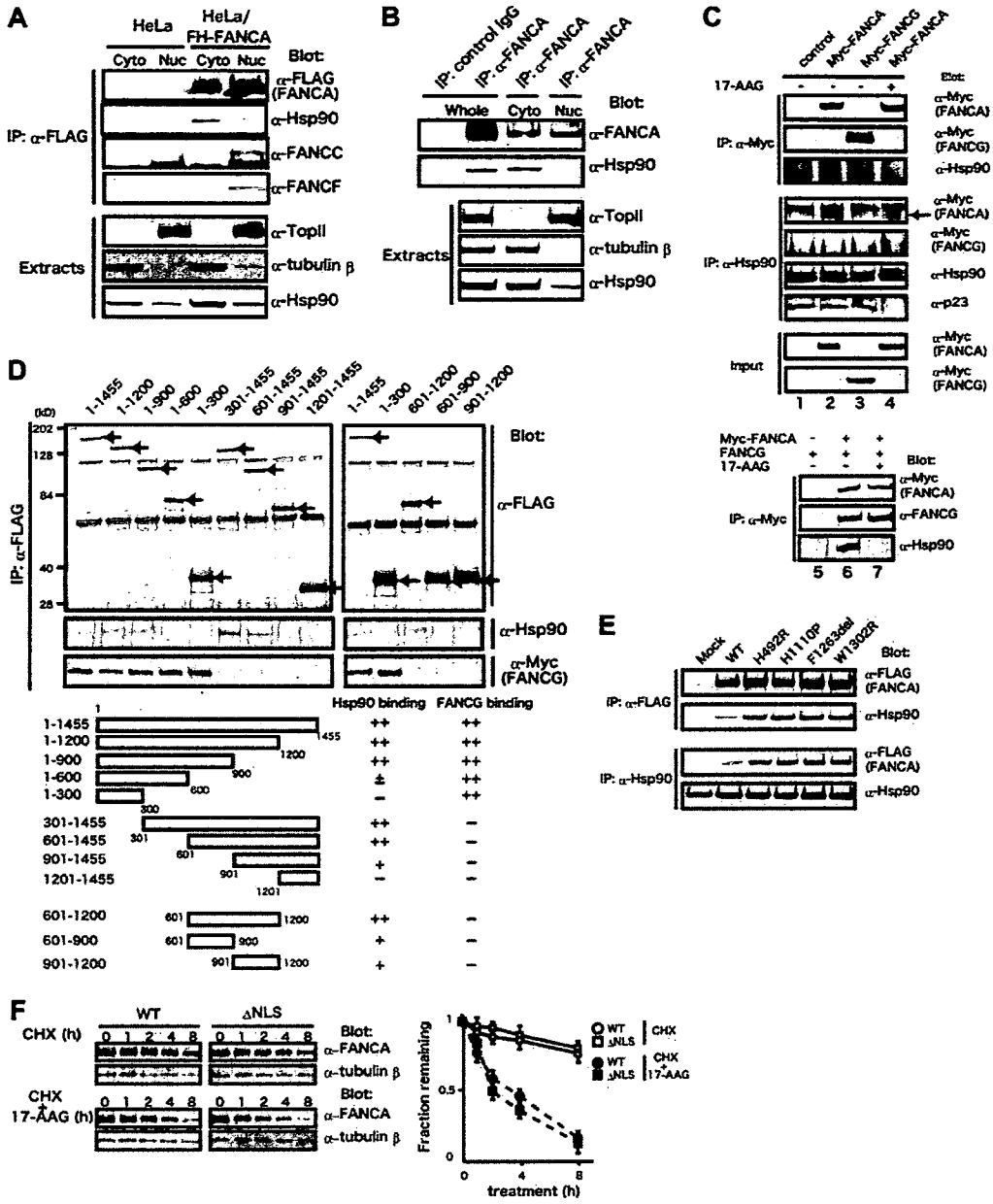

Figure 5. Hsp90 stabilizes cytoplasmic FANCA in a FANCG-independent manner. (A) Cell fractionation study of HeLa/FH-FANCA. Cytoplasmic extracts (Cyto) and nuclear extracts (Nuc) prepared from control HeLa and HeLa/FH-FANCA cells were immunoprecipitated (IP) with anti-FLAG antibody followed by immunoblotting with the indicated antibodies (upper panels). The same extracts were directly immunoblotted with the indicated antibodies (lower panels). Topoisomerase II (Top II) and tubulin-β are nuclear and cytoplasmic markers, respectively. (B) Cell fractionation study of parental HeLa cells. Whole-cell lysates (Whole) and cytoplasmic extracts (Cyto) and nuclear extracts (Nuc), prepared from HeLa cells (1×10^7 cells) were immunoprecipitated with either control rabbit IgG or anti-FANCA antibody, and then immunoblotted with anti-FANCA and anti-Hsp90 antibodies (upper panels). The same extracts were directly immunoblotted with the indicated antibodies (lower panels). Topoisomerase II (Top II) and tubulin-β are nuclear and cytoplasmic markers, respectively. (C) In vitro interaction of FANCA with Hsp90. In vitro transcription/translation reactions were programmed with empty vector (control), pcDNA3 Myc-FANCA (Myc-FANCA), or pcDNA3 Myc-FANCG (Myc-FANCG) in the absence (−) or presence (+) of 10 μM 17-AAG (lanes 1-4). Reaction mixtures were immunoprecipitated with anti-Myc antibody and immunoblotted with the indicated antibodies (upper panels), or immunoprecipitated with anti-Hsp90 antibody and immunoblotted with the indicated antibodies (middle panels). The arrow indicates Myc-FANCA. A portion (10%) of the input material was directly immunoblotted with anti-Myc antibody to detect synthesized FA proteins (lower panels). FANCG was synthesized alone or with Myc-FANCA, in the absence (−) or presence (+) of 10 μM 17-AAG, as described (lanes 5-7). Reaction mixtures were immunoprecipitated with anti-Myc antibody and immunoblotted with the indicated antibodies. (D) Recognition of different regions of FANCA by Hsp90 and FANCG. FANCA full-length protein and deletion mutants with a FLAG-tag at their N-termini were synthesized in vitro. Structures of the deletion mutants are schematically shown at the bottom of the figure. Reaction mixtures were immunoprecipitated with anti-FLAG antibody, followed by immunoblotting with anti-FLAG and anti-Hsp90 antibodies. Arrows indicate synthesized FANCA polypeptides. The same FANCA polypeptides were cosynthesized with Myc-FANCG in vitro, and reaction mixtures were immunoprecipitated with anti-FLAG antibody and immunoblotted with anti-FLAG (data not shown) and anti-Myc antibodies. Results of binding studies are summarized on the right for each mutant (bottom, ranging from negative, −, to strongly positive, ++). (E) Interaction of Hsp90 with FANCA mutants. Lysates from GM6914 cells stably expressing FLAG-tagged wild-type (WT) or mutant FANCA proteins were immunoprecipitated with anti-FLAG antibody (upper panels) or anti-Hsp90 antibody (lower panels) and immunoblotted with the indicated antibodies. (F) Sensitivity of ΔNLS FANCA mutant to 17-AAG. GM6914 cells expressing wild-type FANCA (WT) or ΔNLS mutant were treated with 100 μg/mL CHX alone, (CHX) or with 250 nM 17-AAG (CHX + 17-AAG) for the indicated times. Cell lysates were immunoblotted with anti-FANCA and anti–tubulin-β antibodies. FANCA signals were quantified and normalized against tubulin-β signals. Data represent means ± SE from 3 independent experiments (bottom graph).

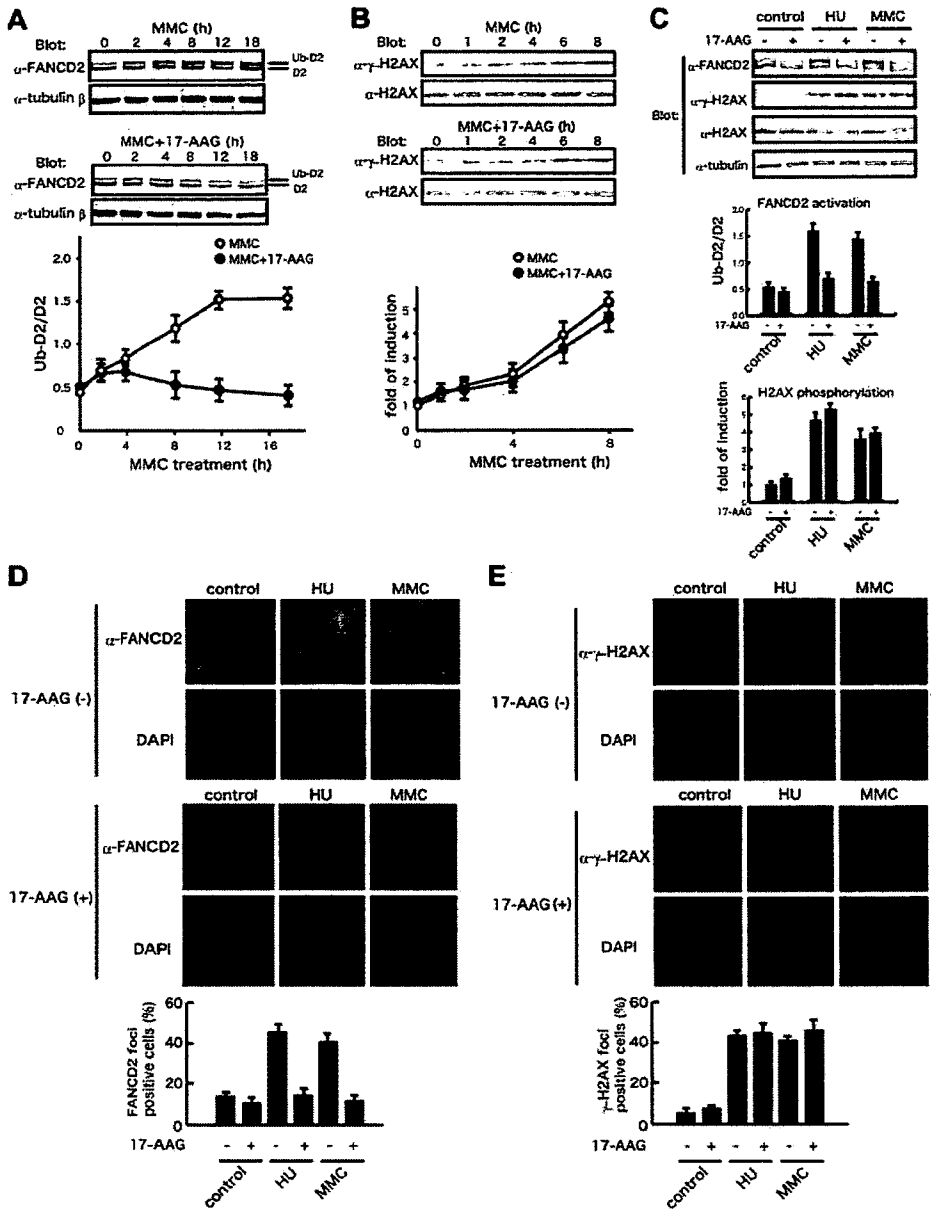

Figure 6. 17-AAG inhibits FANCD2 activation but not H2AX phosphorylation. (A) Effects of 17-AAG on MMC-induced FANCD2 monoubiquitination. HeLa cells were treated with 40 ng/mL MMC alone (MMC) or with 250 nM 17-AAG (MMC + 17-AAG) for the indicated times. Cell lysates were immunoblotted with anti-FANCD2 and anti–tubulin-β antibodies. Protein bands corresponding to FANCD2 (D2) and a monoubiquitinated form of FANCD2 (Ub-D2) were quantified, and ratios of the 2 isoforms (Ub-D2/D2) were determined for each sample. Data represent means ± SE from 3 independent experiments (bottom graph). (B) Effects of 17-AAG on MMC-induced H2AX phosphorylation. HeLa cells were treated with 40 ng/mL MMC alone (MMC) or with 250 nM 17-AAG (MMC + 17-AAG) for the indicated times. Cell lysates were immunoblotted with anti-γ-H2AX and anti-H2AX. Protein bands were quantified and fold inductions of γ-H2AX normalized against H2AX were determined for each sample. Data represent means ± SE from 3 independent experiments (bottom graph). (C) Effects of 17-AAG on FANCD2 monoubiquitination and H2AX phosphorylation in control and HU- and MMC-treated HeLa cells. HeLa cells were treated with 1 mM HU or 40 ng/mL MMC in the absence (−) or presence (+) of 250 nM 17-AAG for 8 hours. Cell lysates were immunoblotted with the indicated antibodies. Ratios of FANCD2 isoforms (Ub-D2/D2) and fold inductions of γ-H2AX normalized against H2AX were determined for each sample as described. Data represent means ± SD from 3 independent experiments. (D-E) Effects of 17-AAG on formation of FANCD2 and γ-H2AX nuclear foci. HeLa cells were treated with 1 mM HU or 40 ng/mL MMC in the absence (−) or presence (+) of 250 nM 17-AAG for 8 hours. Cells were stained with anti-FANCD2 (D) or anti-γ-H2AX (E) antibodies. Cell nuclei were visualized with DAPI staining. In each sample, at least 200 nuclei were examined at original magnification ×200. Nuclei containing more than 10 bright foci were scored as FANCD2- and γ-H2AX foci-positive cells. Data represent means ± SD from 3 independent experiments (bottom graphs). Images were obtained on an Olympus AX70 microscope equipped with UPlan-Apo 20×/0.70 NA and WH 10×/22 objectives (Olympus, Tokyo, Japan) using a PXL charge-coupled device camera (model CH1; Photometrics, Osnabrück, Germany).

phosphorylation of a histone H2A variant H2AX, which is a sensitive marker of DSBs.[54] Immunoblot studies showed that 17-AAG treatment had little effects on MMC- or HU-induced increases of phosphorylated H2AX (γ-H2AX; Figure 6B-C), suggesting that the drug impedes a process from DSB formation to FANCD2 activation. We next studied the effect of 17-AAG on formation of FANCD2 nuclear foci representing recruitment of monoubiquitinated FANCD2 to the chromatin,[25,35] in comparison with formation of γ-H2AX nuclear foci. Consistent with results of the immunoblot studies, 17-AAG treatment markedly suppressed MMC- or HU-induced FANCD2 nuclear focus formation but had little effect on γ-H2AX nuclear focus formation (Figure 6D-E).

The DNA damage-sensitive kinase, ataxia telangiectasia and RAD3-related protein (ATR), is required for DNA damage-induced FANCD2 activation.[55] However, 17-AAG treatment had little effect on ATR activation, as assessed by phosphorylation of Chk1, a substrate of ATR (data not shown), in agreement with previously published data.[11] Collectively, our results suggest that the 17-AAG–induced suppression of FANCD2 activation can be explained by the drug-induced severe reduction and cytoplasmic retention of FANCA.

17-AAG enhances DNA cross-linker–induced cytotoxicity and chromosomal abnormalities

To test whether 17-AAG-induced inactivation of the FA pathway affected cellular sensitivity to DNA cross-linkers, we studied effects of 17-AAG on cisplatin-induced cytotoxicity in HeLa cervical cancer and RPMI8226 myeloma cells. As shown in Figure 7A, 17-AAG sensitized both cells to cisplatin. 17-AAG showed similar effects on MMC-induced cytotoxicity in these cells (data not shown). We next examined whether the effect of 17-AAG on DNA cross-linker–induced cytotoxicity was mediated through suppression of the FA pathway. For this purpose, we studied 17-AAG–induced sensitization to MMC in FANCA-deficient fibroblasts (GM6914) and those complemented by wild-type FANCA

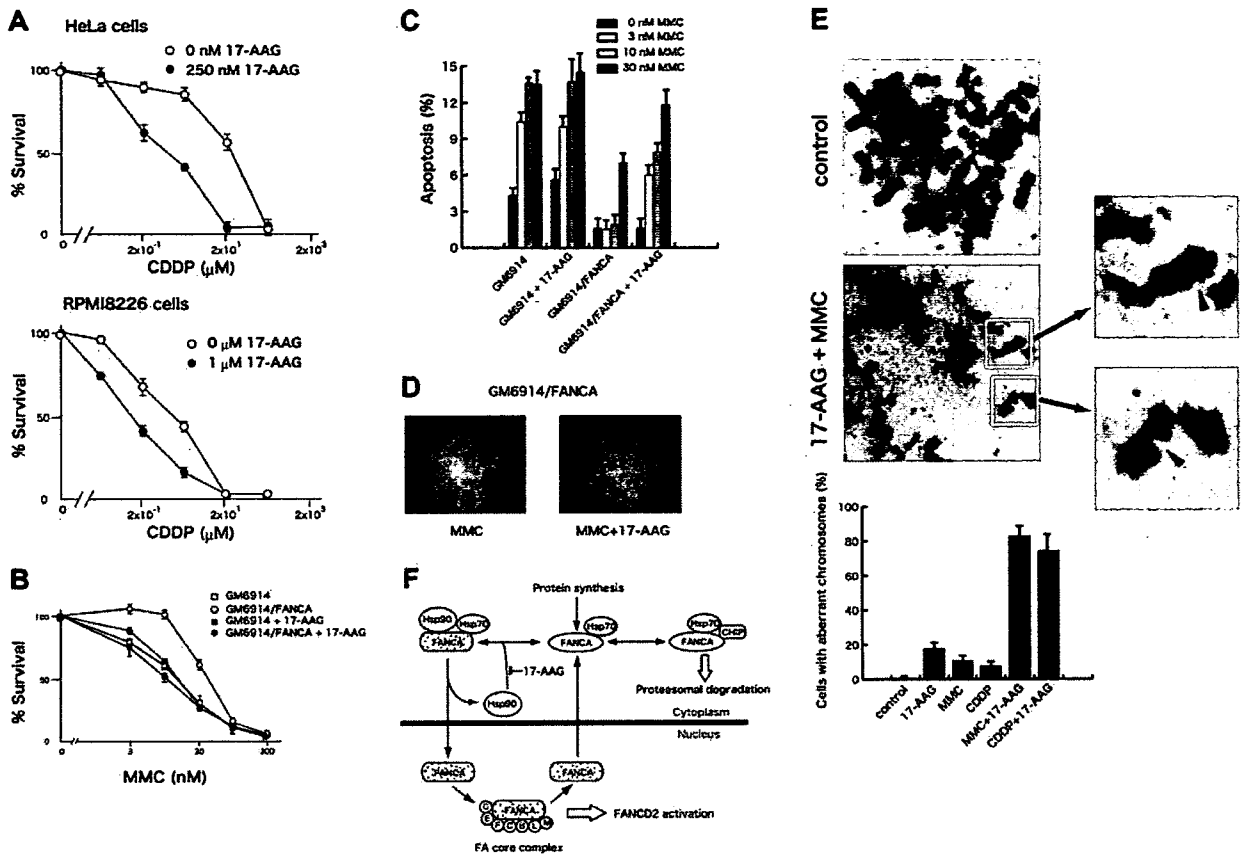

Figure 7. 17-AAG enhances DNA cross-linker–induced cytotoxicity and chromosome abnormalities. (A) HeLa cells were treated with various concentrations of cisplatin (CDDP) alone or with 250 nM 17-AAG for 14 hours. RPMI8226 cells were treated with various concentrations of cisplatin (CDDP) alone or with 1 μM 17-AAG for 20 hours. Cells were washed and then incubated in drug-free culture medium. After 72 hours from the time of initial drug application, cell survival was colorimetrically determined. Data represent means ± SD from triplicate measurements. (B) FANCA-deficient (GM6914) and complemented (GM6914/FANCA) cells were treated with various concentrations of MMC alone or with 250 nM 17-AAG for 14 hours. Cells were washed and incubated in drug-free culture medium. After 72 hours from the time of initial drug application, cell survival was colorimetrically measured. (C-D) FANCA-deficient (GM6914) and complemented (GM6914/FANCA) cells were treated with MMC (0, 3, 10, 30 nM) and 250 nM 17-AAG for 14 hours. Cells were washed and then incubated in drug-free culture medium to complete a total of 40 hours from the time of initial drug application. Apoptotic cells were detected by TUNEL staining. In each sample, at least 400 cells were examined at original magnification ×100, and percentages of apoptotic cells were determined. Data represent means ± SD from triplicate measurements. TUNEL stainings of GM6914/FANCA cells treated with 10 nM MMC alone (MMC) or with 250 nM 17-AAG (MMC + 17-AAG) are shown in panel D. Images were obtained on an Olympus AX70 microscope equipped with UPlanApo 10×/0.40 NA and WH 10×/22 lenses (Olympus) using a PXL charge-coupled device camera (model CH1; Photometrics). (E) HeLa cells were treated with 100 nM MMC or 2 μM cisplatin (CDDP) with or without 250 nM 17-AAG for 24 hours. Cells in metaphase were assessed as aberrant if they presented chromatid breaks. Data represent means ± SD from 3 independent experiments. Arrowheads indicate chromatid breaks. Images were obtained on a Leica DM3000 microscope equipped with HI PLAN 100x/1.25 NA and HC PLAN 10x/22 lenses (Leica, Bensheim, Germany) using a DFC280 digital camera (Leica). (F) A model illustrating how Hsp90 regulates intracellular stability and trafficking of FANCA. FANCA shuttles between the cytoplasm and the nucleus. Cytoplasmic FANCA, newly synthesized and exported from the nucleus, is folded into proper conformation required for nuclear entry by interacting with the Hsp90-based multichaperone complex.[1,2] Hsp90 is probably recycled to form a complex with FANCA in the cytoplasm. The 17-AAG–mediated inhibition of the chaperone cycle promotes proteasomal degradation of FANCA, at least in part, through Hsp70-mediated association with CHIP. In the nucleus, FANCA, -B, -C, -E, -F, -G, -L, and -M are assembled into a multisubunit complex (FA core complex) that is required for FANCD2 activation.

(GM6914/FANCA). As shown in Figure 7B, 17-AAG sensitized GM6914/FANCA cells to MMC-induced cytotoxicity, but this effect was much less pronounced in GM6914 cells. To confirm these results, we determined percentages of apoptotic cells by TUNEL assay (Figure 7C-D). 17-AAG significantly increased MMC-induced apoptotic cells in GM6914/FANCA cells, but this effect was not seen in GM6914 cells (Figure 7C). Together, these results suggest that the effect of 17-AAG depends on the presence of an intact FA pathway.

FA pathway-defective cells characteristically show a high frequency of chromosomal aberrations after exposure to DNA cross-linkers.[14-16] Our results show that chromosome aberrations were detected in a small fraction of HeLa cells after exposure to DNA cross-linkers or 17-AAG, whereas percentages of cells containing chromatid breaks markedly increased after combined treatment with DNA cross-linkers and 17-AAG (Figure 7E). However, radial chromosomes, typical aberrations observed in FA cells, were not detected in these cells. One likely explanation is that Hsp90 inhibition suppresses other DNA repair pathways through which DNA cross-linker–induced DSBs are misrepaired to generate radial chromosomes. [14] To support this notion, activation of DNA-dependent protein kinase, a critical component for nonhomologous end joining, is suppressed by Hsp90 inhibitors. [13]

Discussion

In the present work, we have demonstrated that the Hsp90 chaperone machinery regulates the FA pathway. Our results showed that FANCA associated with Hsp90, in vivo and in vitro, in a 17-AAG–sensitive manner. Furthermore, 17-AAG–mediated disruption of the association between Hsp90 and FANCA induced

rapid proteasomal degradation and cytoplasmic retention of FANCA. Together, these results indicate that FANCA is a client of Hsp90. Because nuclear levels of FANCA have profound effect on FANCD2 activation,[25,27,29,30] the 17-AAG–induced dramatic effects on intracellular turnover and localization of FANCA could be expected to compromise FANCD2 activation. Indeed, 17-AAG markedly suppressed DNA damage-induced monoubiquitination and nuclear focus formation of FANCD2. Furthermore, the drug enhanced cytotoxicity of DNA cross-linkers, apparently in an FA pathway-dependent manner. Even more remarkably, 17-AAG enhanced DNA cross-linker–induced chromosome aberrations. Recent studies suggest that Hsp90 inhibitors sensitize cells to genotoxic agents through depletion of Chk1 and consequent abrogation of cell cycle checkpoint activation. However, since 17-AAG induced similar decreases of Chk1 in FA-defective (GM6914) and complemented (GM6914/FANCA) cells (data not shown), 17-AAG–induced Chk1 depletion is unlikely to explain selective sensitization of the complemented cells. Taken together, our results suggest that Hsp90 is required for full activation of the FA pathway through maintaining intracellular homeostasis of FANCA (Figure 7F), although we cannot exclude the possibility that 17-AAG–induced down-regulation of other FA proteins contribute to suppression of the FA pathway.

As illustrated in our model (Figure 7F), the present work provides several new insights into the regulation of turnover and trafficking of FANCA. First, the disruption of the interaction between Hsp90 and a cytoplasmic fraction of FANCA rapidly induces a large reduction of total cellular levels of FANCA, despite its predominant localization in the nucleus. One explanation is that a nuclear pool of FANCA is rapidly exchangeable with a cytoplasmic pool that is in continuous dynamic cycles of assembly/disassembly with Hsp90 to be protected from proteolysis. To support this notion, nucleocytoplasmic shuttling of FANCA was recently reported.[40] Second, Hsp90 binds and stabilizes cytoplasmic FANCA in a FANCG-independent manner. Although FANCG forms an intermediate subcomplex with FANCA in the cytoplasm,[20,22,27,32] this interaction does not seem critical for stability of cytoplasmic FANCA. FANCG-mediated stabilization of FANCA is probably through promoting the FA core complex formation in the nucleus. Third, our results suggested that Hsp90 inhibition markedly accelerated FANCA degradation through the ubiquitin-proteasome pathway. Our preliminary data suggest that Hsp90 inhibition enhances Hsp70-mediated association between FANCA and CHIP,[6,7,51] which may contribute to proteasomal targeting of FANCA. Finally, Hsp90 is required for nuclear localization of FANCA, although the underlying mechanism remains unknown. Previous studies suggested that N-terminal NLS as well as C-terminus were required for its nuclear localization.[18,27,39] Hence, one likely explanation is that Hsp90-assisted folding of cytoplasmic FANCA is required for the function of NLS or proper conformation of the C-terminal region. An alternative, but not mutually exclusive, explanation is that Hsp90 and its cochaperones link FANCA to the microtubule-based nuclear import machinery, as documented for glucocorticoid receptors and p53.[56,57]

The present findings have important implications for cancer chemotherapy. DNA cross-linkers are a major class of antitumor agents used for standard therapeutics.[58] Increasing evidence suggests that the FA pathway plays an important role in tumor sensitivity to DNA cross-linkers. For example, epigenetic inactivation of *FANCF* by promoter hypermethylation is associated with cisplatin hypersensitivity in primary ovarian cancers, whereas reactivation of the *FANCF* gene causes cross-linker resistance.[59] In another case, enhancement of the FA pathway is involved in melphalan resistance in myeloma cells.[60] Accordingly, pharmacologic inhibition of the FA pathway is expected to sensitize tumor cells to DNA cross-linkers. Recently, Chirnomas et al reported that curcumin inhibits the FA pathway and can be used as a chemosensitizer of cisplatin, although a molecular target of curcumin remains unknown.[61] Geldanamycin analogues are now in clinical trials, and new analogues are being developed.[3,4] In addition, another group of antitumor agents, histone deacetylase inhibitors, induce hyperacetylation of Hsp90, thereby disrupting its chaperone activity.[62-65] These Hsp90 inhibitors are promising for the combined use with DNA cross-linkers. On the other hand, our findings suggest that Hsp90 inhibitors suppress the FA pathway, causing genomic instability in tumor cells, which may lead to malignant progression in vivo. This important question should be addressed in future studies.

Acknowledgments

This work was supported by a Grant-in-Aid for Scientific Research from the Ministry of Education, Science, Technology, Sports and Culture of Japan, and by grants from the Ministry of Health, Labor and Welfare of Japan.

We thank Dr Johan de Winter, Dr Weidong Wang, Dr Maureen Hoatlin, Dr Hiroshi Handa, and Dr Hirokazu Murakami for kindly providing us reagents. We thank Dr Tatsutoshi Nakahata for generous support, Dr Yuko Sato and Dr Miharu Yabe for helpful discussion, and Keiko Nakazato for technical assistance.

Authorship

Contribution: T.O. performed research and wrote the paper; T.H. performed research and analyzed data; H.M. performed research; N.T. analyzed data; and T.Y. designed the research and wrote the paper.

Conflict-of-interest disclosure: The authors declare no competing financial interests.

Correspondence: Takayuki Yamashita, Laboratory of Molecular Genetics, Institute for Molecular and Cellular Regulation, Gunma University, 3-39-15 Showa-machi, Maebashi, Gunma 371-8512, Japan; e-mail: y-taka@showa.gunma-u.ac.jp.

References

1. Pearl LH, Prodromou C. Structure, function, and mechanism of the Hsp90 molecular chaperone. Adv Protein Chem. 2001;59:157-186.
2. Whitesell L, Lindquist SL. HSP90 and the chaperoning of cancer. Nat Rev Cancer. 2005;5:761-772.
3. Neckers L. Chaperoning oncogenes: Hsp90 as a target of geldanamycin. Handb Exp Pharmacol. 2006;172:259-277.
4. Pacey S, Banerji U, Judson I, Workman P. Hsp90 inhibitors in the clinic. Handb Exp Pharmacol. 2006;172:331-358.
5. Schulte TW, Blagosklonny MV, Ingui C, Neckers L. Disruption of the Raf-1-Hsp90 molecular complex results in destabilization of Raf-1 and loss of Raf-1-Ras association. J Biol Chem. 1995;270:24585-24588.
6. Xu W, Marcu M, Yuan X, Mimnaugh E, Patterson C, Neckers L. Chaperone-dependent E3 ubiquitin ligase CHIP mediates a degradative pathway for c-ErbB2/Neu. Proc Natl Acad Sci U S A. 2002;99:12847-12852.
7. Zhou P, Fernandes N, Dodge IL, et al. ErbB2 degradation mediated by the co-chaperone protein CHIP. J Biol Chem. 2003;278:13829-13837.
8. Bagatell R, Beliakoff J, David CL, Marron MT, Whitesell L. Hsp90 inhibitors deplete key anti-apoptotic proteins in pediatric solid tumor cells and demonstrate synergistic anticancer activity with cisplatin. Int J Cancer. 2005;113:179-188.

9. Fedier A, Stuedli A, Fink D. Presence of MLH1 protein aggravates the potential of the HSP90 inhibitor radicicol to sensitize tumor cells to cisplatin. Int J Oncol. 2005;27:1697-1705.
10. Machida H, Matsumoto Y, Shirai M, Kubota N. Geldanamycin, an inhibitor of Hsp90, sensitizes human tumour cells to radiation. Int J Radiat Biol. 2003;79:973-980.
11. Arlander SJ, Eapen AK, Vroman BT, McDonald RJ, Toft DO, Karnitz LM. Hsp90 inhibition depletes Chk1 and sensitizes tumor cells to replication stress. J Biol Chem. 2003;278:52572-52577.
12. Mesa RA, Loegering D, Powell HL, et al. Heat shock protein 90 inhibition sensitizes acute myelogenous leukemia cells to cytarabine. Blood. 2005;106:318-327.
13. Dote H, Burgan WE, Camphausen K, Tofilon PJ. Inhibition of Hsp90 compromises the DNA damage response to radiation. Cancer Res. 2006;66:9211-9220.
14. Niedernhofer LJ, Lalai AS, Hoeijmakers JH. Fanconi anemia (cross)linked to DNA repair. Cell. 2005;123:1191-1198.
15. Levitus M, Joenje H, de Winter JP. The Fanconi anemia pathway of genomic maintenance. Cell Oncol. 2006;28:3-29.
16. Taniguchi T, D'Andrea AD. Molecular pathogenesis of Fanconi anemia: recent progress. Blood. 2006;107:4223-4233.
17. Kupfer GM, Naf D, Suliman A, Pulsipher M, D'Andrea AD. The Fanconi anaemia proteins, FAA and FAC, interact to form a nuclear complex. Nat Genet. 1997;17:487-490.
18. Naf D, Kupfer GM, Suliman A, Lambert K, D'Andrea AD. Functional activity of the Fanconi anemia protein FAA requires FAC binding and nuclear localization. Mol Cell Biol. 1998;18:5952-5960.
19. Yamashita T, Kupfer GM, Naf D, et al. The Fanconi anemia pathway requires FAA phosphorylation and FAA/FAC nuclear accumulation. Proc Natl Acad Sci U S A. 1998;95:13085-13090.
20. Garcia-Higuera I, Kuang Y, Naf D, Wasik J, D'Andrea AD. Fanconi anemia proteins FANCA, FANCC, and FANCG/XRCC9 interact in a functional nuclear complex. Mol Cell Biol. 1999;19:4866-4873.
21. Kruyt FA, Abou-Zahr F, Mok H, Youssoufian H. Resistance to mitomycin C requires direct interaction between the Fanconi anemia proteins FANCA and FANCG in the nucleus through an arginine-rich domain. J Biol Chem. 1999;274:34212-34218.
22. Waisfisz Q, de Winter JP, Kruyt FA, et al. A physical complex of the Fanconi anemia proteins FANCG/XRCC9 and FANCA. Proc Natl Acad Sci U S A. 1999;96:10320-10325.
23. de Winter JP, van der Weel L, de Groot J, et al. The Fanconi anemia protein FANCF forms a nuclear complex with FANCA, FANCC and FANCG. Hum Mol Genet. 2000;9:2665-2674.
24. Garcia-Higuera I, Kuang Y, Denham J, D'Andrea AD. The Fanconi anemia proteins FANCA and FANCG stabilize each other and promote the nuclear accumulation of the Fanconi anemia complex. Blood. 2000;96:3224-3230.
25. Garcia-Higuera I, Taniguchi T, Ganesan S, et al. Interaction of the Fanconi anemia proteins and BRCA1 in a common pathway. Mol Cell. 2001;7:249-262.
26. Medhurst AL, Huber PA, Waisfisz Q, de Winter JP, Mathew CG. Direct interactions of the five known Fanconi anaemia proteins suggest a common functional pathway. Hum Mol Genet. 2001;10:423-429.
27. Adachi D, Oda T, Yagasaki H, et al. Heterogeneous activation of the Fanconi anemia pathway by patient-derived FANCA mutants. Hum Mol Genet. 2002;11:3125-3134.
28. Pace P, Johnson M, Tan WM, et al. FANCE: the link between Fanconi anaemia complex assembly and activity. EMBO J. 2002;21:3414-3423.
29. Meetei AR, de Winter JP, Medhurst AL, et al. A novel ubiquitin ligase is deficient in Fanconi anemia. Nat Genet. 2003;35:165-170.
30. Meetei AR, Levitus M, Xue Y, et al. X-linked inheritance of Fanconi anemia complementation group B. Nat Genet. 2004;36:1219-1224.
31. Meetei AR, Medhurst AL, Ling C, et al. A human ortholog of archaeal DNA repair protein Hef is defective in Fanconi anemia complementation group M. Nat Genet. 2005;37:958-963.
32. Medhurst AL, Laghmani EH, Steltenpool J, et al. Evidence for subcomplexes in the Fanconi anaemia pathway. Blood. Prepublished on May 23, 2006, as DOI 10.1182/blood-2005-11-008151. (Now available as Blood. 2006;108:2072-2080).
33. Yamamoto K, Ishiai M, Matsushita N, et al. Fanconi anemia FANCG protein in mitigating radiation- and enzyme-induced DNA double-strand breaks by homologous recombination in vertebrate cells. Mol Cell Biol. 2003;23:5421-5430.
34. Hussain S, Wilson JB, Medhurst AL, et al. Direct interaction of FANCD2 with BRCA2 in DNA damage response pathways. Hum Mol Genet. 2004;13:1241-1248.
35. Wang X, Andreassen PR, D'Andrea AD. Functional interaction of monoubiquitinated FANCD2 and BRCA2/FANCD1 in chromatin. Mol Cell Biol. 2004;24:5850-5862.
36. Levitus M, Waisfisz Q, Godthelp BC, et al. The DNA helicase BRIP1 is defective in Fanconi anemia complementation group J. Nat Genet. 2005;37:934-935.
37. Levran O, Attwooll C, Henry RT, et al. The BRCA1-interacting helicase BRIP1 is deficient in Fanconi anemia. Nat Genet. 2005;37:931-933.
38. Litman R, Peng M, Jin Z, et al. BACH1 is critical for homologous recombination and appears to be the Fanconi anemia gene product FANCJ. Cancer Cell. 2005;8:255-265.
39. Lightfoot J, Alon N, Bosnoyan-Collins L, Buchwald M. Characterization of regions functional in the nuclear localization of the Fanconi anemia group A protein. Hum Mol Genet. 1999;8:1007-1015.
40. Ferrer M, Rodriguez JA, Spierings EA, de Winter JP, Giaccone G, Kruyt FA. Identification of multiple nuclear export sequences in Fanconi anemia group A protein that contribute to CRM1-dependent nuclear export. Hum Mol Genet. 2005;14:1271-1281.
41. Oda T, Kayukawa K, Hagiwara H, et al. A novel TATA-binding protein-binding protein, ABT1, activates basal transcription and has a yeast homolog that is essential for growth. Mol Cell Biol. 2000;20:1407-1418.
42. Shang L, Tomasi TB. The heat shock protein 90-CDC37 chaperone complex is required for signaling by type I and II interferons. J Biol Chem. 2006;281:1876-1884.
43. de Winter JP, Rooimans MA, van Der Weel L, et al. The Fanconi anaemia gene FANCF encodes a novel protein with homology to ROM. Nat Genet. 2000;24:15-16.
44. Natsume T, Yamauchi Y, Nakayama H, et al. A direct nanoflow liquid chromatography-tandem mass spectrometry system for interaction proteomics. Anal Chem. 2002;74:4725-4733.
45. Hayano T, Yanagida M, Yamauchi Y, Shinkawa T, Isobe T, Takahashi N. Proteomic analysis of human Nop56p-associated pre-ribosomal ribonucleoprotein complexes. Possible link between Nop56p and the nucleolar protein treacle responsible for Treacher Collins syndrome. J Biol Chem. 2003;278:34309-34319.
46. Meetei AR, Sechi S, Wallisch M, et al. A multiprotein nuclear complex connects Fanconi anemia and Bloom syndrome. Mol Cell Biol. 2003;23:3417-3426.
47. Sullivan W, Stensgard B, Caucutt G, et al. Nucleotides and two functional states of hsp90. J Biol Chem. 1997;272:8007-8012.
48. Csermely P, Kajtar J, Hollosi M, et al. ATP induces a conformational change of 90-kDa heat shock protein (hsp90). J Biol Chem. 1993;268:1901-1907
49. Whitesell L, Sutphin PD, Pulcini EJ, Martinez JD, Cook PH. The physical association of multiple molecular chaperone proteins with mutant p53 is altered by geldanamycin, an hsp90-binding agent. Mol Cell Biol. 1998;18:1517-1524.
50. Gooljarsingh LT, Fernandes C, Yan K, et al. A biochemical rationale for the anticancer effects of Hsp90 inhibitors: slow, tight binding inhibition by geldanamycin and its analogues. Proc Natl Acad Sci U S A. 2006;103:7625-7630.
51. McDonough H, Patterson C. CHIP: a link between the chaperone and proteasome system. Cell Stress Chaperones. 2003;8:303-308.
52. Blom E, van de Vrugt HJ, de Vries Y, de Winter JP, Arwert F, Joenje H. Multiple TPR motifs characterize the Fanconi anemia FANCG protein. DNA Repair (Amst). 2004;3:77-84.
53. Rothfuss A, Grompe M. Repair kinetics of genomic interstrand DNA cross-links: evidence for DNA double-strand break-dependent activation of the Fanconi anemia/BRCA pathway. Mol Cell Biol. 2004;24:123-134.
54. Rogakou EP, Pilch DR, Orr AH, Ivanova VS, Bonner WM. DNA double-stranded breaks induce histone H2AX phosphorylation on serine 139. J Biol Chem. 1998;273:5858-5868.
55. Andreassen PR, D'Andrea AD, Taniguchi T. ATR couples FANCD2 monoubiquitination to the DNA-damage response. Genes Dev. 2004;18:1958-1963.
56. Galigniana MD, Harrell JM, O'Hagen HM, Ljungman M, Pratt WB. Hsp90-binding immunophilins link p53 to dynein during p53 transport to the nucleus. J Biol Chem. 2004;279:22483-22489.
57. Harrell JM, Murphy PJ, Morishima Y, et al. Evidence for glucocorticoid receptor transport on microtubules by dynein. J Biol Chem. 2004;279:54647-54654.
58. McHugh PJ, Spanswick VJ, Hartley JA. Repair of DNA interstrand crosslinks: molecular mechanisms and clinical relevance. Lancet Oncol. 2001;2:483-490.
59. Taniguchi T, Tischkowitz M, Ameziane N, et al. Disruption of the Fanconi anemia-BRCA pathway in cisplatin-sensitive ovarian tumors. Nat Med. 2003;9:568-574.
60. Chen Q, Van der Sluis PC, Boulware D, Hazlehurst LA, Dalton WS. The FA/BRCA pathway is involved in melphalan-induced DNA interstrand cross-link repair and accounts for melphalan resistance in multiple myeloma cells. Blood. 2005;106:698-705.
61. Chirnomas D, Taniguchi T, de la Vega M, et al. Chemosensitization to cisplatin by inhibitors of the Fanconi anemia/BRCA pathway. Mol Cancer Ther. 2006;5:952-961.
62. Bali P, Pranpat M, Bradner J, et al. Inhibition of histone deacetylase 6 acetylates and disrupts the chaperone function of heat shock protein 90: a novel basis for antileukemia activity of histone deacetylase inhibitors. J Biol Chem. 2005;280:26729-26734.
63. Kovacs JJ, Murphy PJ, Gaillard S, et al. HDAC6 regulates Hsp90 acetylation and chaperone-dependent activation of glucocorticoid receptor. Mol Cell. 2005;18:601-607.
64. Murphy PJ, Morishima Y, Kovacs JJ, Yao TP, Pratt WB. Regulation of the dynamics of hsp90 action on the glucocorticoid receptor by acetylation/deacetylation of the chaperone. J Biol Chem. 2005;280:33792-33799.
65. Kong X, Lin Z, Liang D, Fath D, Sang N, Caro J. Histone deacetylase inhibitors induce VHL and ubiquitin-independent proteasomal degradation of hypoxia-inducible factor 1alpha. Mol Cell Biol. 2006;26:2019-2028.

Long-term response and outcome following immunosuppressive therapy in thymoma-associated pure red cell aplasia: a nationwide cohort study in Japan by the PRCA collaborative study group

Makoto Hirokawa,[1] Ken-ichi Sawada,[1] Naohito Fujishima,[1] Shinji Nakao,[2] Akio Urabe,[3] Kazuo Dan,[4] Shin Fujisawa,[5] Yuji Yonemura,[6] Fumio Kawano,[7] Mitsuhiro Omine,[8] and Keiya Ozawa,[9] for the PRCA Collaborative Study Group

[1]Division of Hematology and Oncology, Department of Medicine, Akita University School of Medicine, Akita; [2]Department of Cellular Transplantation Biology, Kanazawa University Graduate School of Medicine, Kanazawa, Ishikawa; [3]Division of Hematology, NTT Kanto Medical Center, Shinagawa, Tokyo; [4]Division of Hematology, Third Department of Internal Medicine, Nippon Medical School, Bunkyo, Tokyo; [5]Department of Hematology, Yokohama City University Medical Center, Yokohama, Kanagawa; [6]Department of Transfusion Medicine and Cell TherapyBlood Transfusion Service, Kumamoto University School of Medicine, Kumamoto; [7]National Hospital Organization Kumamoto National Hospital Medical Center, Kumamoto; [8]Internal Medicine, Showa University Fujigaoka Hospital, Yokohama, Kanagawa; and [9]Division of Hematology, Department of Medicine, Jichi Medical School, Kawachi, Tochigi, Japan

Acknowledgments: we thank all physicians of the institutions listed in the Appendix for their contribution to the present study.

Funding: this study was supported by a research grant from the Idiopathic Disorders of Hematopoietic Organs Research Committee of the Ministry of Health, Labour and Welfare of Japan.

Manuscript received April 27, 2007. Manuscript accepted August 16, 2007.

Correspondence:
Makoto Hirokawa, M.D., Ph.D., Division of Hematology and Oncology, Department of Medicine, Akita University School of Medicine, 1-1-1 Hondo, Akita 010-8543, Japan.
E-mail: mhirokawa@hos.akita-u.ac.jp

ABSTRACT

Background
Thymoma-associated pure red cell aplasia (PRCA) accounts for a significant proportion of cases of secondary PRCA and immunosuppressive therapy has been reported to be useful in this condition. However, because of its rarity, the long-term response and relapse rates after immunosuppressive therapy are largely unknown, and optimal management of this disorder remains unclear. The aim of this study was to collect more information on the outcome of patients with thymoma-associated PRCA.

Design and Methods
We conducted a nationwide survey in Japan. From a total of 185 patients, comprising 73 with idiopathic and 112 with secondary PRCA, 41 patients with thymoma were evaluated for this report. End-points of this study were the response rate, duration of the response after immunosuppressive therapy and overall survival.

Results
Surgical removal of thymoma was reported in 36 patients, 16 of whom developed PRCA at a median of 80 months post-thymectomy. First remission induction therapy was effective in 19 of 20 patients treated with cyclosporine, 6 of 13 patients treated with corticosteroids and 1 of 1 treated with cyclophosphamide. No cyclosporine-responders relapsed within a median observation period of 18 months (range; 1 to 118 months). Relapse of anemia was observed in three corticosteroid-responders who did not receive additional cyclosporine. Only two patients were in remission after stopping therapy for 19 and 67 months. The estimated median overall survival time of all patients was 142 months.

Conclusions
Thymoma-associated PRCA showed an excellent response to cyclosporine and cyclosporine-containing regimens were effective in preventing relapse of anemia. It does, however, remain uncertain whether cyclosporine can induce a maintenance-free hematologic response.

Key words: pure red cell aplasia, thymoma, cyclosporine.

Citation: Hirokawa M, Sawada K, Fujishima N, Nakao S, Urabe A, Dan K, Fujisawa S, Yonemura Y, Kawano F, Omine M, Ozawa K for the PRCA Collaborative Study Group. Long-term response and outcome following immuno-suppressive therapy in thymoma-associated pure red cell aplasia: a nationwide cohort study in Japan by the PRCA collaborative study group. Haematologica. 2008 Jan; 93(1):27-33. DOI: 10.3324/haematol.11655

Introduction

Acquired pure red cell aplasia (PRCA) is an anemic condition characterized by the absence of reticulocytes in blood and the absence of erythroid precursors in the bone marrow.[1-4] Other hematopoietic cell lineages are present with no evident morphological abnormalities. Secondary PRCA is associated with various underlying diseases including lymphoproliferative disorders, thymoma, solid tumors, autoimmune diseases, drugs and viral infections.[1,2] The association of PRCA with thymoma was first described in 1928 by Matras and Priesel,[1] and thymoma-associated PRCA accounts for a significant proportion of the secondary cases.[5,6] Thymoma-associated PRCA is generally thought to be an organ-specific autoimmune disease as well as an idiopathic form, and immunosuppressive therapy, including corticosteroids, cyclophosphamide and cyclosporine, has been reported to be useful.[5,7,8,9] Thompson *et al.* recently reported their 50-year single institution experience with 13 patients with thymoma-associated PRCA,[10] and showed that surgical resection of the thymoma was insufficient to induce normalization of erythropoiesis, and that anti-thymocyte globulin was an effective adjuvant treatment but associated with high treatment-related morbidity due to frequent infectious complications. However, the optimal management of thymoma-associated PRCA and the long-term outcome after immunosuppressive therapy remain unclear because of the rarity of this disorder.

The efficacy and long-term outcome after immunosuppressive therapy for secondary PRCA could differ according to the underlying diseases. To date, the overall long-term response and relapse rates after immunosuppressive therapy in acquired PRCA are largely unknown. We, therefore, conducted a nationwide survey to investigate the current status of immunosuppressive therapy for acquired chronic PRCA based on a relatively large cohort of patients in Japan. This report is a summary focusing on immunosuppressive therapy for thymoma-associated PRCA.

Design and Methods

Data collection and patients' characteristics

The first questionnaires were sent to 109 hematology departments in Japan to estimate the number of patients aged 15 and above who had been newly diagnosed as having acquired PRCA between 1990 and 2006. Patients with human parvovirus B19 infection-associated PRCA were excluded. Eligible patients were limited to those who had been diagnosed during this period in order to minimize the effect of transfusion-associated hepatitis C virus infection. Overall, 273 patients were enrolled from 45 institutions. Secondary questionnaires were then sent to these institutions to collect data regarding underlying diseases, laboratory findings including peripheral blood cell counts and leukocyte differentials, results of bone marrow examination, immunological and cytogenetic parameters, efficacy of immunosuppressive therapy and outcome. Morphological diagnosis of bone marrow was done by hematologists at each institution. Of the 185 patients identified, 73 patients were classified as having idiopathic PRCA and 112 as having secondary PRCA.

Table 1. Co-morbidity in patients with thymoma-associated PRCA (n=41).

Underlying diseases	*Number of patients*
Autoimmune disease	11
Myasthenia gravis	6
Systemic lupus erythematosus	1
Mixed connective tissue disease	1
Dermatomyositis	1
Polyneuropathy	1
Autoimmune hemolytic anemia	1
Malignancy	5
Myelodysplastic syndrome	1
Stomach	1
Breast	1
Thyroid	1
Bladder	1

The classification of PRCA was based on the criteria proposed by the Hematopoietic Organs Research Committee of the Ministry of Health, Labor and Welfare of Japan in 2005.[11] This classification was fundamentally based on the criteria proposed by Dessypris and Lipton.[2] Forty-two patients had both thymoma and PRCA. One patient who had undergone autologous hematopoietic stem cell transplantation for recurrent malignant thymoma before the onset of PRCA was excluded from this study, so 41 patients were finally selected for analysis of thymoma-associated PRCA. Personal identifying information was protected by giving each data set a unique patient number at each participating institution. This study was approved by the institutional review board, and performed according to the Declaration of Helsinki and the Ethical Guidelines for Epidemiological Research of the Ministry of Education, Culture, Sports, Science and Technology and the Ministry of Health, Labor and Welfare of Japan.

The age of the patients at the onset of PRCA ranged from 27 to 82 years (median age, 66 years) and there was a 3:4 male to female ratio of cases. Autoimmune diseases and malignancies were complications in 11 and five patients, respectively (Table 1). Thymoma histology was varied with one case of type A, nine type AB, three type B1, and four type B2 cases according to the WHO classification of histological typing of tumors of the thymus.[12] Hyperplasia was reported in one case, and histological subtypes could not be determined in 23 cases. The hemoglobin concentration ranged from 2.7 to 10.9 g/dL with a median of 5.8 g/dL.

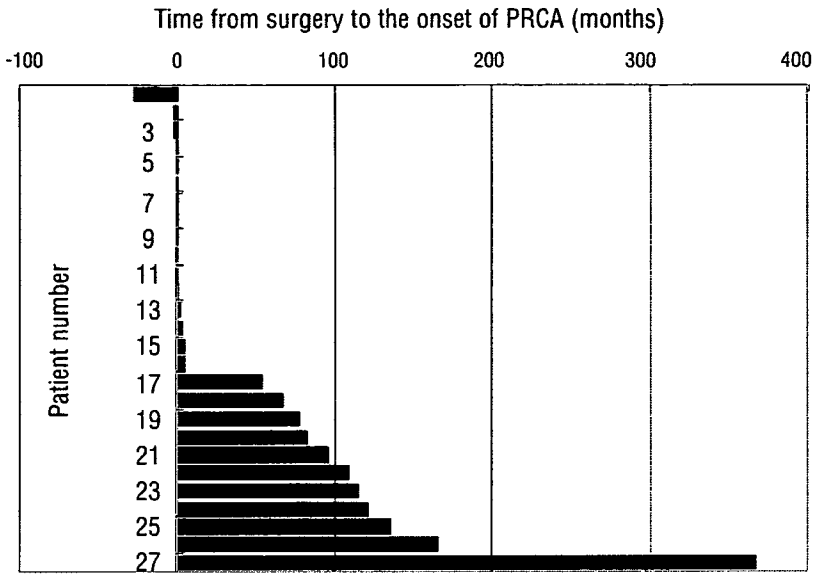

Figure 1. Chronological sequence of surgical removal of the thymoma and the onset of PRCA. The time when each patient underwent surgery is located at point 0 on the x-axis. Data were available for 27 patients.

Table 2. The first remission induction therapy for thymoma-associated PRCA.

	N.	*CR*	*PR*	*NR*	*Response rate*
Cyclosporine	20	16	3	1	19/20 (95%)
Corticosteroids	13	5	1	7	6/13 (46%)
Cyclophosphamide	1	1			1/1 (100%)
Anabolic steroid	1			1	0/1 (0%)
None	6				

Definition of the responses and data analysis

Complete remission (CR), partial remission (PR) and no response (NR) were defined as the achievement of normal hemoglobin levels without transfusion, the presence of anemia but without transfusion dependence, and continued dependence on transfusions, respectively. The date of remission was defined as that of the final transfusion after the initiation of remission induction therapy. The minimum period required for evaluation of response to agents was set at 2 weeks; therefore, agents added within 2 weeks were included into a simultaneous combination with the preceding agents. In some analyses, the patients were classified according to the agent used for maintenance therapy, e.g. a cyclosporine group and a non-cyclosporine group, regardless of the agents used successfully to induce remission. The agents for remission induction and salvage therapy were divided into those used initially and those used either sequentially or in a later combination, respectively. The agent for maintenance therapy was defined as that used or tapered off after successful induction of remission. Relapse was defined as the reappearance of transfusion requirement. Survival was estimated using the Kaplan-Meier method and the significance of differences was calculated by the log-rank test. The end-points of this study were the response rate, duration of the response to immunosuppressive therapy and overall survival. Secondary endpoints included the time from surgical removal of the thymoma to the onset of PRCA.

Results

Surgical removal of the thymoma

Thymomectomy was performed in 36 patients, while four patients did not undergo surgery. Data on surgery were not available for one patient. The chronological sequence of thymoma removal and the onset of PRCA could be analyzed in 27 of the 36 patients: the thymoma was resected before the onset of PRCA in 16 patients, with the anemia developing a median of 80 months after surgery (range; 1 to 366 months) (Figure 1). Eleven patients underwent surgery after the diagnosis of PRCA. In the remaining nine patients, the time of surgery was unknown.

Five patients underwent surgery without any adjuvant therapy: two of these patients had no response, while the clinical response was unknown in the other three patients.

Rate of response to the first remission induction therapy

The initial treatment for these patients included cyclosporine (n=20), corticosteroids (n=13), cyclophosphamide (n=1) and an anabolic steroid (n=1) Six patients did not receive any medication (Table 2).

Cyclosporine produced CR or PR in 19/20 patients

Table 3. Effective salvage therapy for patients who failed to respond to the first remission induction therapy.

UPN	Remission induction therapy			Salvage therapy	
	Initial agent	Response (@ days)	Discontinuation	Agent	Response
125	Methyl-PSL PSL	NR (105)	Yes No	CsA	CR
37	PSL	NR (250)	No	CsA	PR
99	FK506 PSL	NR (75)	Yes No	CsA	CR
44	Anabolic steroid	NR (125)	Yes	CsA	PR

PSL: prednisolone; CsA: cyclosporine A; CR: complete remission; PR: partial remission; NR: no response.

(95%). The patients who responded to cyclosporine had histological type A, type AB and type B1 thymoma. The median initial dose of cyclosporine for the responding patients was 4.6 mg/kg body weight (b.w.) with a range from 2.0 to 6.3 mg/kg b.w. The non-responding patient was given 3.9 mg/kg b.w. of cyclosporine. All evaluable cyclosporine-responders (n=15) became independent of blood transfusions within 2 weeks after starting treatment (*data not shown*).

Corticosteroids produced CR or PR in 6/13 patients (46%). The median initial doses of corticosteroids for the responding and non-responding patients were 1.0 mg/kg b.w. (range, 0.3 to 1.1 mg/kg) and 0.8 mg/kg (range, 0.3 to 1.2 mg/kg), respectively. Three evaluable corticosteroid-responders became independent of transfusions 0, 9 and 135 days after starting therapy. Three of six corticosteroid-responders were given additional cyclosporine and were maintained in CR (n=2) and PR (n=1).

Cyclophosphamide was administered to one patient who had a complete response. The time to response from the start of therapy was unknown. The one patient treated with an anabolic steroid did not achieve a clinical response.

Salvage therapy for non-responders to the first remission induction therapy

The patient who failed to respond to initial cyclosporine therapy did not receive any other immunosuppressive treatment, and continued to receive transfusions. Of the seven patients who failed to respond to the initial corticosteroid therapy, five were then treated with cyclosporine therapy, resulting in a response in three of these patients. These three patients were continuously given corticosteroids after starting cyclosporine (Table 3). One patient who failed to respond to the initial treatment with an anabolic steroid was given cyclosporine and achieved a PR.

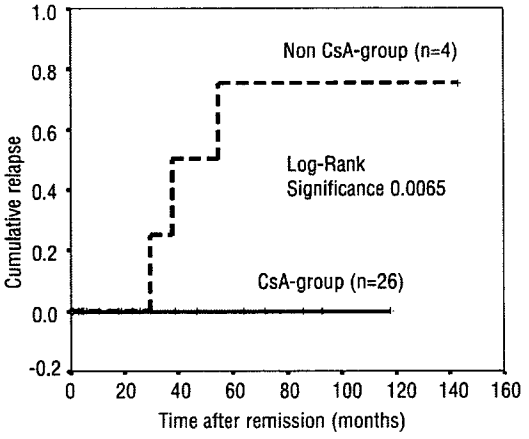

Figure 2. Cumulative incidence of relapse following immunosuppressive therapy in thymoma-associated PRCA. Relapse was defined as the reappearance of transfusion requirement. The cyclosporine-group (CsA-group) consisted of the following patients; 19 patients who had responded to the initial cyclosporine therapy, 3 patients who responded to corticosteroid therapy followed by additional cyclosporine, and four patients who received cyclosporine as salvage therapy. There was a significant difference in the duration of the response between the two groups based on the log-rank test ($p<0.01$).

Duration of the response and overall survival

There were no relapses among the 19 patients who responded to the first remission induction therapy with cyclosporine (median observation period of 18 months; range, 1 to 118 months). Three corticosteroid-responders were given additional cyclosporine and were maintained in continuous remission. In contrast, relapse of anemia was observed in three other corticosteroid-responders who did not receive cyclosporine. The patient who responded to cyclophosphamide has remained in CR for 19 months after stopping treatment. There were no relapses among the four patients who failed to respond to the first remission induction therapy but responded to salvage treatment with cyclosporine (Table 3).